A network diagram consisting of various-sized light blue circles connected by thin white lines, set against a solid blue background. The circles are scattered across the page, with some larger and some smaller, creating a complex web of connections.

Joint Research Programme
BTO 2023.047 | June 2023

PFAS in sea-spray aerosols

Report

PFAS in sea-spray aerosols

BTO 2023.047 | June 2023

This research is part of the Joint Research Programme of KWR, the water utilities and Vewin.

Project number

402045/270 and 403977

Project manager

Patrick Bauerlein

Client

BTO - Thematical research - Chemical safety

Authors

Elvio Amato, Frederic Béen, Dennis Vughs

Quality Assurance

Thomas ter Laak

Sent to

This report is distributed to BTO-participants and is public.

Keywords

PFAS; sea-spray aerosols; air sampling; duineninfiltratie

Year of publishing
2023

More information

Dr Elvio Amato
T +31(0)646950231
E elvio.amato@kwrwater.nl

PO Box 1072
3430 BB Nieuwegein
The Netherlands

T +31 (0)30 60 69 511
E info@kwrwater.nl
I www.kwrwater.nl

KWR

June 2023 ©

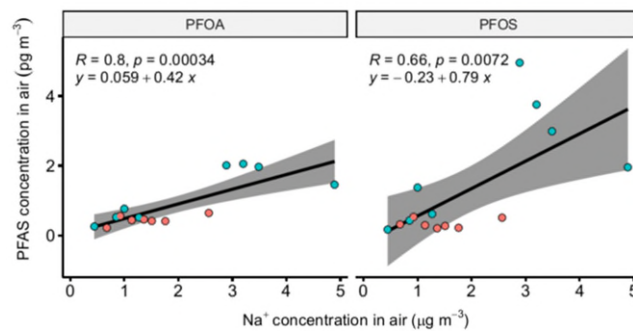
All rights reserved by KWR. No part of this publication may be reproduced, stored in an automatic database, or transmitted in any form or by any means, be it electronic, mechanical, by photocopying, recording, or otherwise, without the prior written permission of KWR.

Managementsamenvatting

PFAS uit sea-spray aerosolen dragen bij aan luchtverontreiniging in kustgebieden, nader onderzoek nodig om risico voor drinkwatervoorziening in te schatten

Auteurs: Elvio Amato, Frederic Béen, Dennis Vughes.

Poly- en perfluoralkylstoffen (PFAS) zijn alomtegenwoordig in het milieu en komen consequent voor in waterbronnen die voor de productie van drinkwater worden gebruikt. De meeste PFAS-bronnen worden in verband gebracht met antropogene activiteiten, maar PFAS zijn ook aangetroffen in gebieden waar geen direct verband kan worden gelegd met industriële en/of stedelijke activiteiten. Recentelijk zijn sea-spray aerosolen (SSA) in verband gebracht met PFAS-verontreiniging in de atmosfeer. PFAS in lucht blijkt verband te houden met de aanwezigheid van SSA, zo blijkt uit onderzoek op twee locaties die relevant zijn voor drinkwaterproductie. Nader onderzoek naar de depositie en processen in de bodem is nodig om de risico's voor de drinkwaterproductie goed in te schatten.



Relaties tussen PFAS en Na⁺ concentraties gemeten in luchtmonsters verzameld in Wijk aan Zee (groen) en Nes (rood).

Belang: evaluatie van SSA als potentiële bron van PFAS-verontreiniging bij duininfiltratie

In de literatuur gerapporteerde laboratoriumstudies hebben aangetoond dat SSA bijdragen aan de overdracht van PFAS van zeewater naar de atmosfeer, en als gevolg daarvan kunnen SSA een belangrijke bron van PFAS-transport en -verspreiding over de hele wereld zijn, met mogelijke gevolgen voor drinkwaterproductielocaties nabij de kust (en mogelijk ook in het binnenland). Het is dus belangrijk te weten welke rol SSA spelen bij PFAS-verontreiniging van kustgebieden voor drinkwaterproductie.

Aanpak: bemonstering van SSA en karakterisering van PFAS- en tracerionenconcentraties

Het voorkomen van PFAS in de lucht is onderzocht op twee kustlocaties in Nederland: Wijk aan Zee en

Ameland. In Wijk aan Zee vindt duininfiltratieplaats voor drinkwaterproductie, op Ameland wordt daarvoor grondwater gewonnen. Op beide locaties werd een hoog-volume luchtmonsternemer ingezet voor het verzamelen van luchtmonsters: 7 monsters op Ameland tijdens de lente en 8 monsters in Wijk aan Zee tijdens winter en zomer (2022). De luchtmonsters werden onderzocht op correlaties tussen PFAS en tracer-ionen zoals Na⁺. Deze laatste werden gebruikt als indicatoren voor de omvang van SSA in het bestudeerde gebied. Aan de kust werden ook 3 zeewatermonsters geanalyseerd ter vergelijking met PFAS-concentraties in de lucht en voor het inschatten van verrijdingsfactoren in SSA. PFAS metingen zijn uitgevoerd met een door KWR gevalideerde LC-(HR)MS methode.

Resultaten: PFAS worden consequent aangetroffen in luchtmonsters en houden verband met SSA

PFAS werden consequent gemeten in de op beide locaties verzamelde luchtmonsters, in concentraties tot ~ 5 pg/m³. De samenstelling van PFAS was over het algemeen zeer consistent, ongeacht de bemonsteringslocatie en het seizoen, wat suggereert dat een vergelijkbare bron van PFAS deze locaties heeft beïnvloed. PFOA en PFOS waren de meest voorkomende PFAS en kwamen doorgaans voor in concentraties die driemaal zo hoog waren als die van andere PFAS met uitzondering van 6:2 FTS, dat af en toe in een vergelijkbare concentratie voorkwam). De wintermonsters uit Wijk aan Zee bevatten hogere concentraties (typisch 2 tot 7 keer, afhankelijk van de verbinding) dan de zomermonsters, wat wijst op mogelijke seizoenen dynamiek. De PFAS-concentraties in Ameland (lente) waren over het algemeen consistent met die in Wijk aan Zee in de zomer. Lineaire regressieanalyse wees op algemene significante relaties tussen PFAS- en Na⁺-concentraties in luchtmonsters, wat suggereert dat de PFAS-verontreiniging in de lucht waarschijnlijk verband hield met SSA. Door gegevens te combineren van PFAS die op alle locaties en in alle bemonsteringsperioden werden aangetroffen, werden statistisch significante verbanden gevonden met Na⁺ voor PFHxA, PFHpA, PFOA, PFNA, PFHxS en PFOS, terwijl geen significante relaties werden gevonden voor PFBS, PFDA and 6:2 FTS. Er werden ook statistisch significante verbanden gevonden tussen de PFAS-concentraties en de windsnelheid (een mogelijk gevolg van een verhoogde SSA-productie), terwijl de windrichting geen invloed leek te hebben op de PFAS-concentraties in de lucht. De PFAS-concentraties in zeewater waren doorgaans < 3,5 ng/L en vaak onder de detectiegrens (1 ng/L),

alleen werd op Ameland 12 ng/L PFOS aangetroffen. De samenstelling van PFAS in SSA was zeer vergelijkbaar met die in zeewatermonsters (vooral voor PFSA), wat de hypothese ondersteunt dat atmosferische PFAS op deze locaties via de vorming van SSA uit zee afkomstig zijn. Schattingen van verrijksfactoren laten zien dat de PFAS-belasting in SSA tussen ~ 20 en ~ 4000 maal groter kan zijn dan die in zeewater, wat erop wijst dat PFAS zeer efficiënt van zeewater naar lucht worden overgebracht.

Eerdere Nederlandse studies hebben laten zien dat het voorkomen van zeezout (dat nauw samenhangt met SSA) in de lucht niet beperkt blijft tot kustgebieden zodat depositie van PFAS uit SSA voor het hele land relevant kan zijn.

Implementatie: verder onderzoek naar de depositie van SSA in kustgebieden

Dit onderzoek bevestigt de rol van SSA in de PFAS belasting van kustgebieden, met mogelijke doorwerking op de bronnen voor drinkwatervoorziening en kustnabije natuur. We weten nog niet hoe representatief de metingen zijn voor langere periodes en grotere gebieden, en hoe groot de PFAS-voorraad in de zee is. Ook moeten de PFAS-transportmechanismen in de bodem worden beoordeeld om het effect van SSA-depositie op drinkwaterbronnen in te schatten. Nader onderzoek is nodig om hier duidelijkheid over te krijgen, zodat drinkwaterbedrijven weten wat er op ze afkomt en daarop kunnen anticiperen.

Rapport

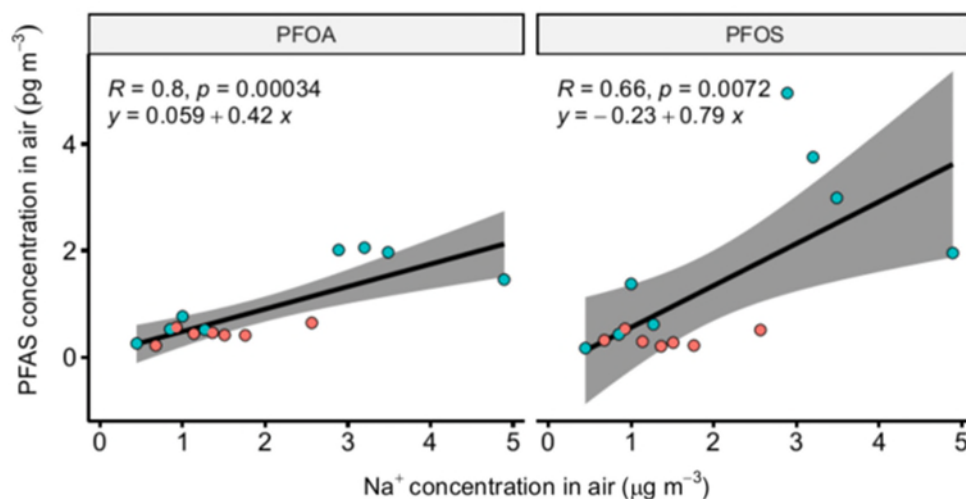
Dit onderzoek is beschreven in het rapport *PFAS in sea-spray aerosols* (BTO 2023.047).

Management summary

PFAS in sea-spray aerosols

Authors: Elvio Amato, Frederic Béen, Dennis Vughs.

Poly- and perfluoroalkyl substances (PFAS) are ubiquitous in the environment and consistently occur in water sources used for drinking water production. Most PFAS sources are associated with anthropogenic activities, however, PFAS have also been found in areas where no direct link can be established with industrial and/or urban activities. Recently, sea-spray aerosols (SSA) have been linked to PFAS contamination in the atmosphere. PFAS in air appears to be related to the presence of SSA, according to research at two sites relevant to drinking water production. Further investigations of deposition and transport in soil are needed to properly assess the risks to drinking water production.



Relationships between PFAS and Na⁺ concentrations measured in air samples collected in Wijk aan Zee (green) and Nes (red)

Scope: characterization of SSA as a potential source of PFAS contamination in coastal areas

Laboratory studies reported in the literature have shown that SSA contributes to the transfer of PFAS from seawater to the atmosphere, and as a result, SSA may be a major source of PFAS transport and distribution around the world, with potential impacts on drinking water production sites near the coast (and possibly inland). It is therefore important to know the role of SSA in PFAS contamination in coastal areas and to evaluate the risk this may pose to drinking water production.

Method: sampling of SSA and characterization of PFAS and tracer ions concentrations

The occurrence of PFAS in air was investigated at two coastal locations in the Netherlands: Wijk aan Zee and Ameland. At Wijk aan Zee, dune infiltration takes place for drinking water production, while at Ameland groundwater is extracted for this purpose. At both locations, a high-volume air sampler was used to collect aerosol samples (i.e., 7 samples in Ameland during spring and 8 samples in Wijk aan Zee during winter and summer, respectively). The aerosol samples were examined for correlations between PFAS and tracer ions such as Na⁺. Tracer ions are used as indicators of the occurrence and amount of SSA in

the studied area. On the coast, 3 seawater samples were also analysed for comparison with PFAS concentrations in SSA and for estimating water-to-air enrichment factors. PFAS measurements were performed using an LC-(HR)MS method validated by KWR.

Results: PFAS were consistently found in air samples and linked to SSA

PFAS were consistently measured in the aerosol samples collected at both sites, in concentrations up to ~ 5 pg/m^3 . PFAS composition was generally very consistent, irrespective of sampling location and season, suggesting that a similar source of PFAS affected these locations. PFOA and PFOS were the most abundant PFAS and generally occurred at concentrations more than three times higher than those of other PFAS (with the exception of 6:2 FTS, which occasionally occurred at a similar concentration). The winter samples from Wijk aan Zee contained higher concentrations (typically 2 to 7 times, depending on the compound) than the summer samples, indicating possible seasonal dynamics. PFAS concentrations in Ameland (spring) were generally consistent with those in Wijk aan Zee in summer. Linear regression analysis indicated overall significant relationships between PFAS and Na^+ concentrations in aerosol samples, suggesting that PFAS pollution in air was probably related to SSA. The relationship between Na^+ and PFAS was typically stronger in samples from Wijk aan Zee than those from Ameland: this may be due to the relatively small sample size and short sampling period investigated in Ameland. Combining data from PFAS found at all sites and in all sampling periods, statistically significant relationships were found with Na^+ for PFHxA, PFHpA, PFOA, PFNA, PFHxS and PFOS, while weak or no relationships were found for PFBS, PFDA and 6:2 FTS. Statistically significant relationships were also found between PFAS concentrations and wind speed (a possible cause of increased SSA production), while wind direction did not seem to affect PFAS concentrations in air. PFAS concentrations in seawater were generally < 3.5 ng/L and often below the detection limit of the method (1 ng/L), except for PFOS in Ameland which was found at a concentration of 12 ng/L . The composition of PFAS in SSA was very similar to that in seawater samples (especially for PFSA), supporting the hypothesis that atmospheric PFAS at these sites originated from the

sea via the formation of SSA. Estimations of enrichment factors indicated that the PFAS burden in SSA can be between ~ 20 and ~ 4000 times greater than that in seawater, suggesting that PFAS are very efficiently transferred from seawater to air. Previous studies in the Netherlands have shown that the occurrence of SSA in air is not limited to coastal areas only, and this indicates that the potential impact of PFAS from SSA may be relevant for the whole country.

Implementation: further investigation of SSA deposition in coastal areas

This research confirms that SSA contribute to the load of PFAS in coastal zones, with possible effects on sources of drinking water supply and coastal wildlife. It is currently unclear how representative the measurements are for longer periods and larger areas, and how large the PFAS 'stock' in the sea is. PFAS transport mechanisms in soil also need to be assessed to estimate the potential effect of SSA deposition on drinking water sources. Further research is needed to clarify this, so that drinking water companies can estimate and prevent potential risks.

The Report

This research is reported in report *PFAS in sea-spray aerosols* (BTO-2023.047).

Contents

<i>Management summary</i>	5
Contents	7
1 Introduction	8
1.1 Purpose	8
1.2 Objectives	8
2 Material and methods	9
2.1 Chemicals and reagents	9
2.2 Sampling of sea-spray aerosols	9
2.3 Sample preparation and analysis	11
2.4 Instrumental analysis	11
2.5 Data analysis	11
3 Results and discussion	12
3.1 PFAS concentrations in air particulate	12
3.1.1 Wijk aan Zee	12
3.1.2 Nes	13
3.2 Na ⁺ and Mg ²⁺ concentrations in air particulate	14
3.3 Relationships between PFAS and Na ⁺ concentrations	15
3.4 Influence of wind direction and speed	17
3.5 Concentrations in seawater	19
3.6 PFAS enrichment in SSA	20
3.7 Indicative estimates of SSA deposition	21
4 Conclusions	22
References	23
Appendix I	26

1 Introduction

1.1 Purpose

Per- and polyfluoroalkyl substances (PFASs) are a diverse group of persistent chemicals that are widely found in environmental samples (Lai et al., 2019; Melake et al., 2022; Tang et al., 2022; Weber et al., 2017; Zhao et al., 2016) (Appendix I). Recent studies have highlighted the role of sea-spray aerosols (SSA) in atmospheric transport of PFAS and its contribution to the global spreading of these substances (Casas et al., 2020; H. Johansson et al., 2019; Sha et al., 2022). SSA are a suspension of particles in air which is generated by bubble bursting at the interface between air and seawater. Air is introduced in seawater by breaking waves, forming bubbles that rise towards the surface and burst. Bubble bursting results in the formation of film drops and jet drops of size typically ranging from less than 1 μm to more than 100 μm (de Leeuw et al., 2011). Laboratory studies have shown that transfer of PFAS from water to air may occur following SSA formation (H. Johansson et al., 2019; Reth et al., 2011). During this process, a considerable enrichment of PFAS has been observed from seawater to SSA, which has been attributed to absorption of PFAS in air bubbles during their transport to the surface (Cao et al., 2019; Casas et al., 2020; H. Johansson et al., 2019; Sha et al., 2021). Enrichment occurs due to the surface-active properties of PFAS, which enhances their adsorption at the air-water interface (Oppo et al., 1999). These factors are generally estimated using PFAS concentration ratios between SSA and seawater, normalized by tracer ions concentrations (e.g., Na^+ and Mg^{2+}) measured in the corresponding media. Enrichment appears to be linked to the length of the fluorinated carbon chain of PFAS, i.e., PFAS with a number of carbons > 7 show greater the enrichment factors (H. Johansson et al., 2019; Sha et al., 2021). In addition, tracer ion concentrations can be used to link PFAS concentrations to SSA, i.e., a positive correlation between PFAS and tracer ions concentrations in air samples may indicate that SSA are a relevant source of PFAS in the atmosphere (Sha et al., 2022). The chemical structure of PFAS is characterized by an apolar, linear or branched per- or polyfluorinated carbon chain often terminated in a polar functional group, such as carboxylic or sulfonic acid as in the case of legacy PFAS (Appendix I). Due to their high solubility in water, in particular for short chains, and poor degradation in the environment, these substances may reach drinking water sources and pose a risk to human health (Ateia et al., 2019; Balgooyen and Remucal, 2022; Cousins et al., 2016; Podder et al., 2021; Sharma et al., 2016; Sunderland et al., 2019). There are multiple sources that may contribute directly or indirectly to PFAS contamination in drinking water. For instance, landfills leachate (Hamid et al., 2018) and desorption from contaminated soil may contribute to increasing PFAS concentrations in groundwater (Ahrens et al., 2015; Cousins et al., 2016; Van Leeuwen et al., 2023; Weber et al., 2017), and desorption from sediment (Balgooyen and Remucal, 2022; Langberg et al., 2020) and emissions from anthropogenic activities may lead to contamination of surface water (Balgooyen and Remucal, 2022). Atmospheric deposition has also been identified as a source of PFAS contamination in the environment (Casal et al., 2017; Sammut et al., 2017; Shimizu et al., 2021; Young et al., 2007).

1.2 Objectives

In this study, we investigated the occurrence of PFAS in SSA in two coastal locations in the Netherlands, i.e., Wijk aan Zee and Nes (Ameland), used for drinking water production. This is a first step into characterising the potential contribution of SSA to PFAS contamination in coastal areas (soil and groundwater) that are not directly affected by anthropogenic activities. This project was conducted in coordination with another study (DPWE – Lot van PFAS in duinen) aiming at investigating PFAS occurrence in soil and groundwater in one of the locations where SSA measurements were performed (i.e., Wijk aan Zee). It is hypothesised that deposition of SSA on soil may contribute to contamination in groundwater used for drinking water production at facilities located on the Dutch coast and Wadden Islands. The results of this study contribute to a more comprehensive characterization of PFAS contamination sources and their potential impact on current and future PFAS concentrations in drinking water.

2 Material and methods

2.1 Chemicals and reagents

All chemicals were analytical-reagent-grade or equivalent analytical purity. Organic solvents (i.e., acetone and methanol) and ammonium hydroxide solution were purchased from Merck and Sigma Aldrich, respectively. Ultrapure water (UP) was utilised for sample preparation and analysis ($18.2 \text{ M}\Omega \text{ cm}^{-1}$). Target analytes included perfluoro-n-butanoic acid (PFBA), perfluoro-n-pentanoic acid (PFPeA), perfluoro-n-hexanoic acid (PFHxA), perfluoro-n-heptanoic acid (PFHpA), perfluoro-n-octanoic acid (PFOA), perfluoro-n-nonanoic acid (PFNA), perfluoro-n-decanoic acid (PFDA), perfluoro-n-undecanoic acid (PFUnDA), perfluoro-n-dodecanoic acid (PFDoDA), perfluoro-n-tridecanoic acid (PFTrDA), perfluoro-n-tetradecanoic acid (PFTeDA), 4:2 fluorotelomer sulfonic acid (4:2 FTS), 6:2 fluorotelomer sulfonic acid (6:2 FTS), 8:2 fluorotelomer sulfonic acid (8:2 FTS), hexafluoropropylene oxide dimer acid (HFPO-DA), 4,8-dioxa-3H-perfluorononanoic acid (NaDONA), 9-chlorohexadecafluoro-3-oxanonane-1-sulfonic acid (9Cl-PF3ONS), 11-chloroeicosafuoro-3-oxaundecane-1-sulfonic acid (11Cl-PF3OUdS), perfluoro-n-butanefluorobutanesulfonic acid (PFBS), perfluoropentane sulfonic acid (PFPeS), perfluoro-n-hexanesulfonic acid (PFHxS), perfluoro-n-heptanesulfonic acid (PFHpS), perfluoro-n-octanesulfonic acid (PFOS), perfluoro-n-nonane sulfonic acid (PFNS), perfluoro-n-decanesulfonic acid (PFDS), perfluoro-1-butanefluorobutanesulfonamide (FBSA), perfluoro-1-hexanesulfonamide (FHxSA), perfluoro-1-octanesulfonamide (FOSA), N-methylperfluorooctanesulfonamidoacetic acid (N-MeFOSAA), and N-ethylperfluorooctanesulfonamidoacetic acid (N-EtFOSAA). Ultrashort-chain PFAS such as trifluoromethanesulfonamide (PFMeSA), pentafluoroethanesulfonamide (PFEtSA), trifluoroacetic acid (TFA), trifluoromethanesulfonic acid (F3-MSA), perfluoropropanoic acid (PFPrA), and perfluoroethane sulfonic acid (PFEtSA) were measured in the follow-up BO project 404465/001 and results reported in a memo (in progress). Mass labelled internal standard (IS) consisting of a mixture of 19 carboxylic and sulphonic PFAS were purchased from Wellington Laboratories (Ontario, Canada). The IS HFPO-DA- $^{13}\text{C}_3$ was supplied by Greyhound Chromatography and Allied Chemicals (Birkenhead, United Kingdom).

2.2 Sampling of sea-spray aerosols

Sea-spray aerosols were collected using a high-volume particulate sampler (MicroPNS HVS01, Umwelttechnik MCZ, Germany) equipped with a PM10 head (Figure 1) specifically purchased for this project. SSA were retained on a quartz fibre filter of dimension $203 \times 254 \text{ mm}$ (MK-360, Munktell). Filters were heated at $900 \text{ }^\circ\text{C}$ overnight prior to exposure. Measurements were performed using a flow rate of $68 \text{ m}^3/\text{h}$ for a duration of 48 h. The sampling device was deployed in two locations in the Netherlands, i.e., in the PWN dune-infiltration site of Wijk aan Zee (WZ), and in the Vitens production site in Nes (NE), Ameland, at approximately 800 and 350 m from the sea shore, respectively (Figure 1; additional pictures available in Appendix I). Sampling was performed in 3 different seasons of the year (2022). Measurements were carried out in winter (February, WZ1-4) and summer (i.e., July-August, WZ5-8), in Wijk aan Zee, and in spring (April-May), in Nes (NE1-7), respectively. Seven measurements were performed at each location, and a total of 3 field blanks were collected (2 in Wijk aan Zee and 1 in Nes, respectively). Field blanks were obtained by loading filters on the device for 30 seconds without starting the device. In Wijk aan Zee, 4 additional parallel measurements were performed in winter using a high-volume air sampler (Sierpa Instruments, USA) provided by Stockholm University. This allowed to compare measurements performed using different devices. Except for this comparison, only data obtained using the sampler from KWR are further discussed in the report. After exposure, filters were carefully wrapped in aluminium foil and stored at $4 \text{ }^\circ\text{C}$ until analysis. During SSA measurements, seawater samples were collected at each location (500 mL) and stored frozen until analysis. Data relative to atmospheric parameters (e.g., temperature, humidity, wind direction, wind speed, precipitation duration and amount, etc.) were collected from the Royal Netherlands Meteorological Institute (KNMI) (<http://www.knmi.nl/nederland-nu/klimatologie/daggegevens>).

Sampling of SSA occurred during different seasons and under varying atmospheric conditions, which were measured for each sampling event and location (Appendix I). Measurements for Wijk aan Zee were obtained from two stations (Wijk aan Zee and IJmuiden) because not all parameters were available at the closest station. For Nes, atmospheric parameters were collected from the nearest station located in Terschelling.

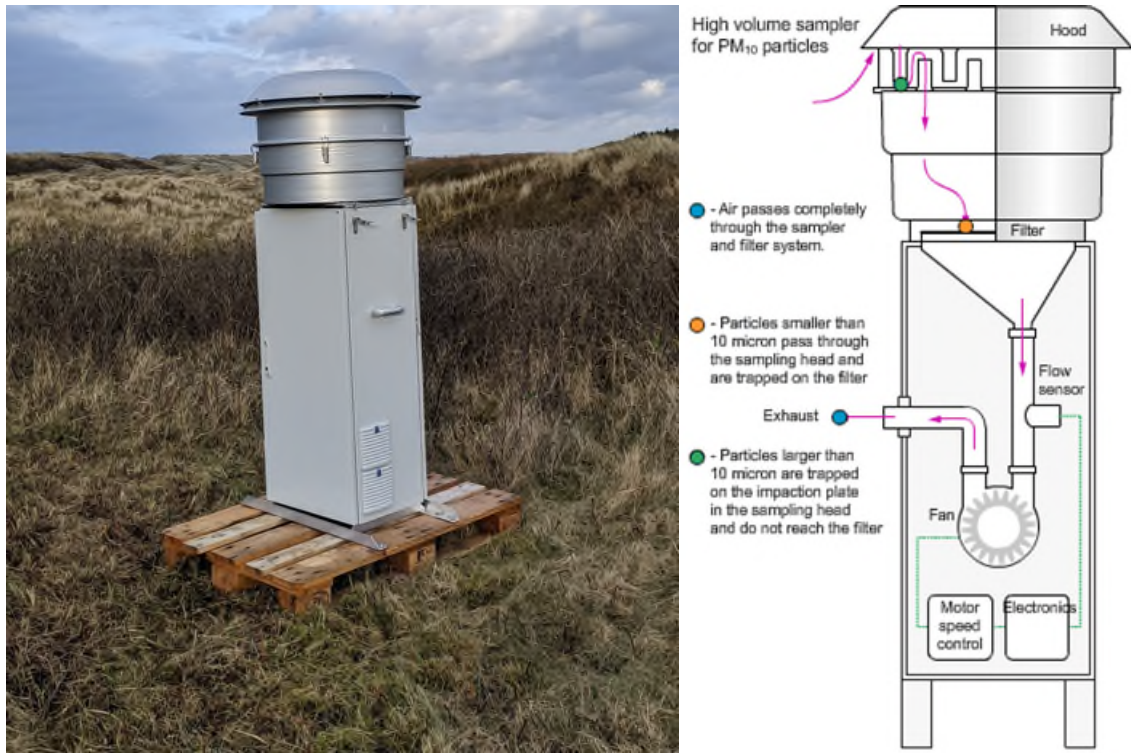


Figure 1. Picture and schematic of the high-volume air sampler used for collecting air particulate.



Figure 2. Sampling locations used for measurements of PFAS in air particulate of the Dutch coast (Wijk aan Zee) and islands (Ameland).

2.3 Sample preparation and analysis

Prior to extraction, filters were sliced in half, and each halve transferred into a clean polypropylene (PP) tube. Two or three portions of filter (6 mm diameter each) were punched and stored in plastic tubes for metal analysis. After addition of internal standard (IS), 35 mL of methanol were added to each tube and samples sonicated for 90 min at 60 °C. The extract was transferred into a clean tube, and the procedure was repeated two more times. The combined extracts were reduced to approximately 10 mL under a gentle flow of N₂ heated at 80 °C. Samples were centrifuged for 10 min at 3500 rpm, and the supernatant blown down to 500 µL. Before injection, samples were brought to a final volume of 1000 µL using ultra-pure water and filtered (0.45 µm). PFAS concentrations in seawater samples (500 mL), including field blanks, were determined using a method developed in the BTO 402045-153 (*PFAS – Bedreiging voor de waterketen*), which was based on solid-phase extraction (SPE) using weak anion exchange (WAX) cartridges (150 mg, 30 µm, 6cc, Oasis®). The portions of filter previously punched were extracted for Na⁺ and Mg²⁺ analysis by sonicating samples in 3 mL UP water for 15 minutes followed by centrifugation at 4000 rpm for 10 min. The supernatant was transferred to a clean tube and analysed by means of inductively coupled plasma-mass spectrometry (ICPMS, Thermo iCAP TQ). Air particulate concentrations were expressed as the mass of PFAS (pg) or Na⁺ (µg) extracted from filters divided by the volume of air sampled (m⁻³). Seawater sample (one for each sampling event) were extracted following a protocol based on solid-phase extraction (SPE) using weak anion exchange (WAX) cartridges (150 mg, 30 µm, 6cc, Oasis®). Na⁺ and Mg²⁺ concentrations in seawater were measured by means of ICPMS.

2.4 Instrumental analysis

PFAS concentrations in air particulate and water samples were determined using liquid chromatography coupled with high resolution mass spectrometry (LC-HRMS). Chromatographic separations was achieved using a Vanquish ultrahigh-performance liquid chromatography system (ThermoFisher Scientific, Breda, the Netherlands) equipped with an XBridge® BEH C18 (2.5 µm, 2.1 x 100 mm Column XP, Waters), and the mass spectrometer used was an Orbitrap FusionTMTribridTMmass (Thermo Fisher Scientific). The injection volume and the flow rate were 10 µL and 0.3 mL/min, respectively. Initial eluent composition was A: 5 mM NH₄Ac in UP-water and B: 5 mM NH₄Ac in MeOH. Calibration standards were prepared in 50:50 MeOH:UP-water %(v/v) at concentration levels of 0, 0.25, 0.50, 1, 2.5, 10, 25, 50 µg/L.

Field blanks were analysed for PFAS, Na⁺ and Mg²⁺ concentrations. Average concentrations are expressed as mean ± standard deviation, and were calculated only when a substance was detected in at least 70% of the observations. When less than 70% of the measurements were above the limit of quantification (LOQ), average concentrations are reported as semiquantitative. Half the LOQ was used for concentrations <LOQ for which no peak integration was achievable.

2.5 Data analysis

Linear correlations between variables were investigated using the Pearson correlation coefficient (*R*). Prior to calculation of the Pearson correlation coefficient, data were tested for normality (Shapiro-Wilk's test). Differences in total PFAS concentrations measured in the different locations and time of the year were investigated using analysis of variance (ANOVA) followed by Tukey's test. Data were tested for normality of residuals distribution (Shapiro-Wilk's test) and for homogeneity of variance (Levene's test) prior to hypothesis testing. Unless otherwise stated, the level of significance α was 0.05. This means that statistical significance can be inferred if the calculate *p*-value is lower than 0.05.

3 Results and discussion

3.1 PFAS concentrations in air particulate

3.1.1 Wijk aan Zee

Several PFAS were measured in samples collected in winter in Wijk aan Zee, including PFCAs (PFPeA, PFHxA, PFHpA, PFOA, PFNA, PFDA), PFASs (PFBS, PFHxS, PFHpS, PFOS), and other PFAS (6:2 FTS, FOSA and HFPO-DA) (Figure 3). PFCAs and PFASs had a number of carbon atoms ranging between 7 and 10, and between 4 and 8, respectively. Average PFAS concentrations were generally lower than 0.5 pg m^{-3} , except for PFOA and PFOS which occurred at greater concentrations (i.e., 1.87 ± 0.28 and $3.41 \pm 1.27 \text{ pg m}^{-3}$ ($n = 4$), respectively). Except for PFOA and PFOS, these results were consistent with previous measurements conducted in the Arctic (Wong et al., 2018), which indicated average concentrations generally ranging between 0.1 and 1 pg m^{-3} , and in Norway, where concentrations were typically $< 1 \text{ pg m}^{-3}$ (Sha et al., 2022) (Annex I). In contrast, concentrations were generally higher than those measured in the Antarctic region (typically $< 0.05 \text{ pg m}^{-3}$, except for PFBA which occurred at $\sim 1.7 \text{ pg m}^{-3}$) (Casas et al., 2020). However, PFAS concentrations in air samples appear to show large temporal variability and may vary over several orders of magnitude within months (Sha et al., 2022; Wong et al., 2018).

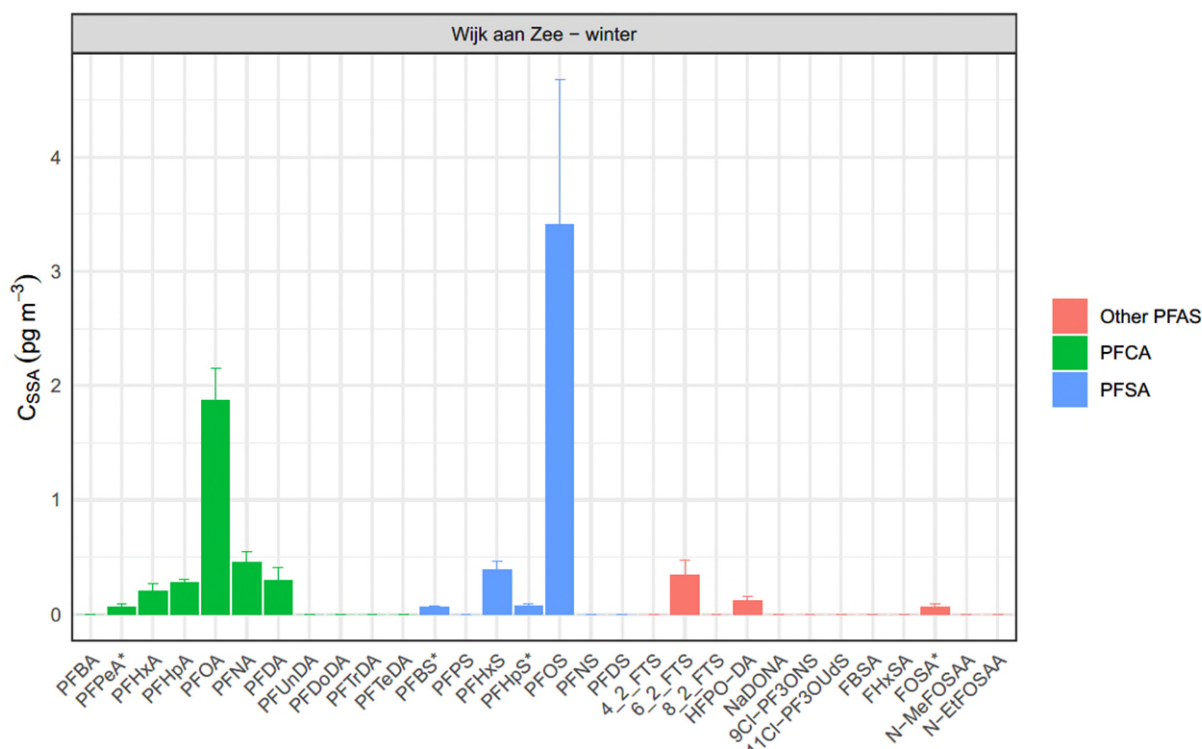


Figure 3. PFAS concentrations in air particulate samples collected in winter in Wijk aan Zee (mean \pm SD, $n = 4$). Asterisks indicate semi-quantitative results.

In summer, concentrations were typically lower than those measured in winter (Figure 4). Almost the same PFCA and PFSA were detected in summer, except for PFPeA, PFHxA, PFHpS, FOSA and HFPO-DA which were found only in samples collected in winter. For compounds that were quantitatively measured (i.e., PFHpA, PFOA, PFNA, PFDA and

PFOS) ratios between concentrations measured in summer and in winter ranged between 0.19 and 0.35, suggesting that the decrease in PFAS concentrations measured in air particulate in summer was relatively consistent among different compounds. When considering total PFAS concentrations (i.e., sum of all PFAS measured at concentrations > LOQ), significant differences were observed between samples collected in winter and summer ($p < 0.0001$). Overall, these results suggest that seasonal variation in PFAS concentrations in air particulate may be expected at this location. The fluorotelomer 6:2 FTS and HFPO-DA were consistently measured in samples from Wijk aan Zee in winter, whereas in summer, only 6:2 FTS was detected. 6:2 FTS is a fluorotelomer commonly found in aqueous film-forming foam (AFFF) (Thai et al., 2022; Wu et al., 2022), whilst HFPO-DA is a perfluoroether carboxylic acid more recently introduced as a replacement of conventional PFAS (Mullin et al., 2019; Yang et al., 2022).

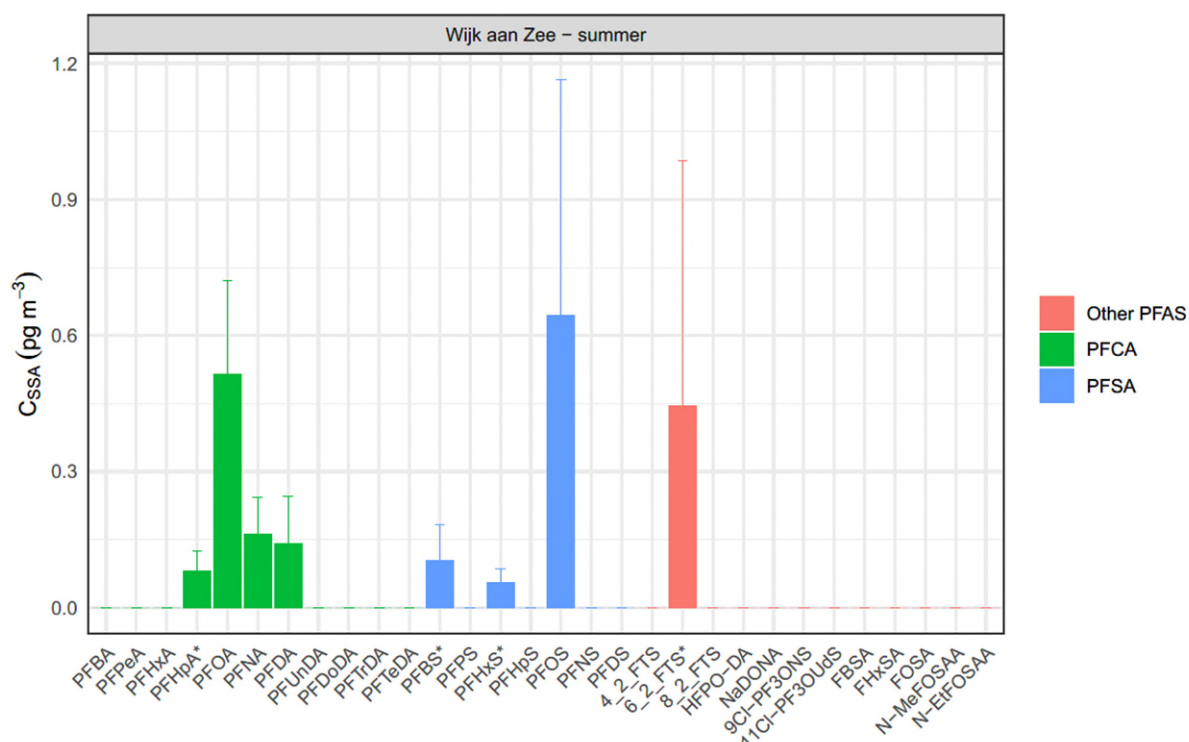


Figure 4. PFAS concentrations in air particulate samples collected in summer in Wijk aan Zee (mean \pm SD, $n = 4$). Asterisks indicate semi-quantitative results.

3.1.2 Nes

Air samples collected in Nes showed a very similar PFAS composition to those measured in Wijk aan Zee (Figure 5). Concentrations were very consistent with those measured in samples collected in summer in Wijk aan Zee, and considerably lower than those measured in winter ($p < 0.0001$, based on total concentrations). PFOA and PFOS were the compounds occurring at the highest concentrations, i.e., approximately 2-fold greater than other PFAS. The consistency in PFAS composition observed between location and time of the year may indicate that these locations were affected by the same source of atmospheric PFAS. PFAS concentrations in this location were overall consistent with those measured in a previous study in Norway, and showed a similar bell-like distribution indicating increasing concentrations from C5 to C8 and decreasing concentrations from C8 to C11 (Appendix I) (Sha et al., 2022). A similar trend was also observed in samples from Wijk aan Zee collected in winter (Figure 3). The amount of PFAS transferred from seawater to the atmosphere depends on their concentrations in the water and their enrichment factors. This could be due to the greater enrichment factors observed for increasing number of carbon atoms (H. Johansson et al., 2019; Sha et al., 2021), and typically lower concentrations found in the North Sea for PFAS with a number of carbons > 8 (Muir and Miaz, 2021).

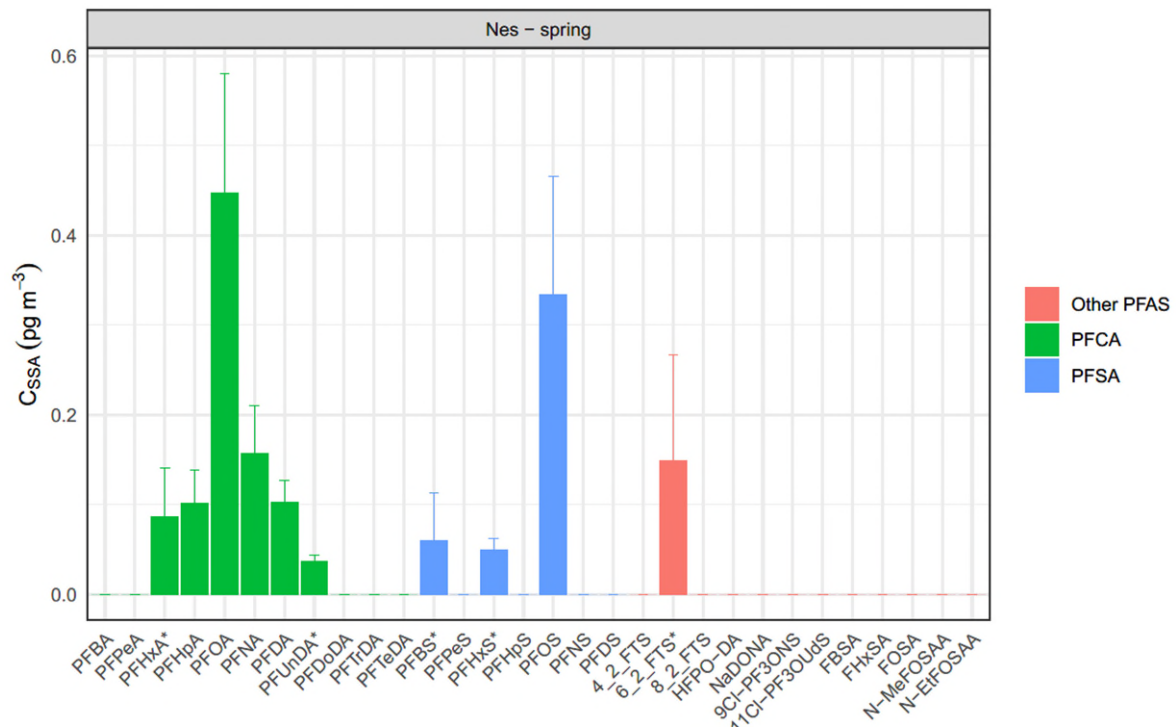


Figure 5. PFAS concentrations in air particulate samples collected in spring in Nes (mean \pm SD, $n = 7$). Asterisks indicate semi-quantitative results.

3.2 Na^+ and Mg^{2+} concentrations in air particulate

Measurements of ions such as Na^+ and Mg^{2+} in air samples can indicate the presence of SSA in the atmosphere. Correlations between these tracer ions and PFAS have been used to link PFAS contamination in the atmosphere with SSA (Sha et al., 2022). In this study, Na^+ and Mg^{2+} were found in all samples of air particulate. In Nes, Na^+ concentrations ranged between 0.67 and 2.5 $\mu\text{g}/\text{m}^3$, whereas in Wijk aan Zee, concentrations ranged between 0.45 and 1.3 $\mu\text{g}/\text{m}^3$, and 2.9 and 4.9 $\mu\text{g}/\text{m}^3$ for the summer and winter sampling, respectively. Concentrations measured in Wijk aan Zee in winter were on average 2.5 and 4 times higher than those measured in Nes and Wijk aan zee in summer, respectively. This may indicate seasonal variations in SSA formation in the atmosphere. Na^+ and Mg^{2+} concentrations were strongly correlated ($p = 2.2 \times 10^{-16}$, $R = 1$) (Figure 6), and the slope of the linear regression (0.120) was consistent with those previously measured in two locations in Norway (0.135 and 0.141, respectively) (Sha et al., 2022). In addition, $\text{Mg}^{2+}/\text{Na}^+$ ratios found in SSA (0.123 ± 0.006 , $n = 15$) were consistent with those found in seawater samples collected at these locations (0.131 ± 0.001 , $n = 3$) and with literature values (Culkin and Cox, 1966; Sha et al., 2022).

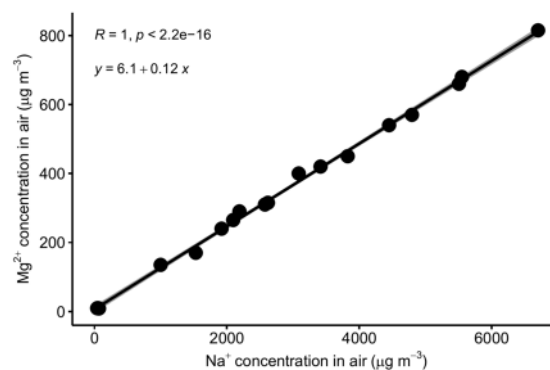


Figure 6. Relationships between Na^+ and Mg^{2+} concentrations in air particulate samples. The strength of the correlation is estimated by the Pearson correlation coefficient R (max = 1), and the statistical significance of the correlation is indicated by the p -value. Shaded areas indicate confidence intervals of the correlation coefficient at 95%.

3.3 Relationships between PFAS and Na⁺ concentrations

Correlations between tracer ions such as Na⁺ and Mg²⁺ and PFAS concentrations in air samples can be used to link PFAS to SSA and infer whether SSA were a major source of PFAS in the atmosphere. Since Na⁺ and Mg²⁺ were strongly correlated, and Na⁺ is the most abundant tracer in seawater, only relationships between PFAS and Na⁺ are discussed here. A previous study has shown that PFAS concentrations in air samples were positively correlated with Na⁺ concentrations at one location in the north of Norway, although these correlations were overall weaker and significant only for PFOA and PFNA in a second location investigated in the south of the country (Sha et al., 2022). Due to the relatively large data variability and small sample size, relationships between PFAS and Na⁺ concentrations in samples from Wijk aan Zee were investigated by combining data obtained from both winter and summer measurements, and focusing on compounds that were found in both sampling events. PFAS concentrations were significantly and positively correlated with Na⁺ concentrations, except for PFBS, 6:2 FTS, PFOS, and PFDA (Figure 7).

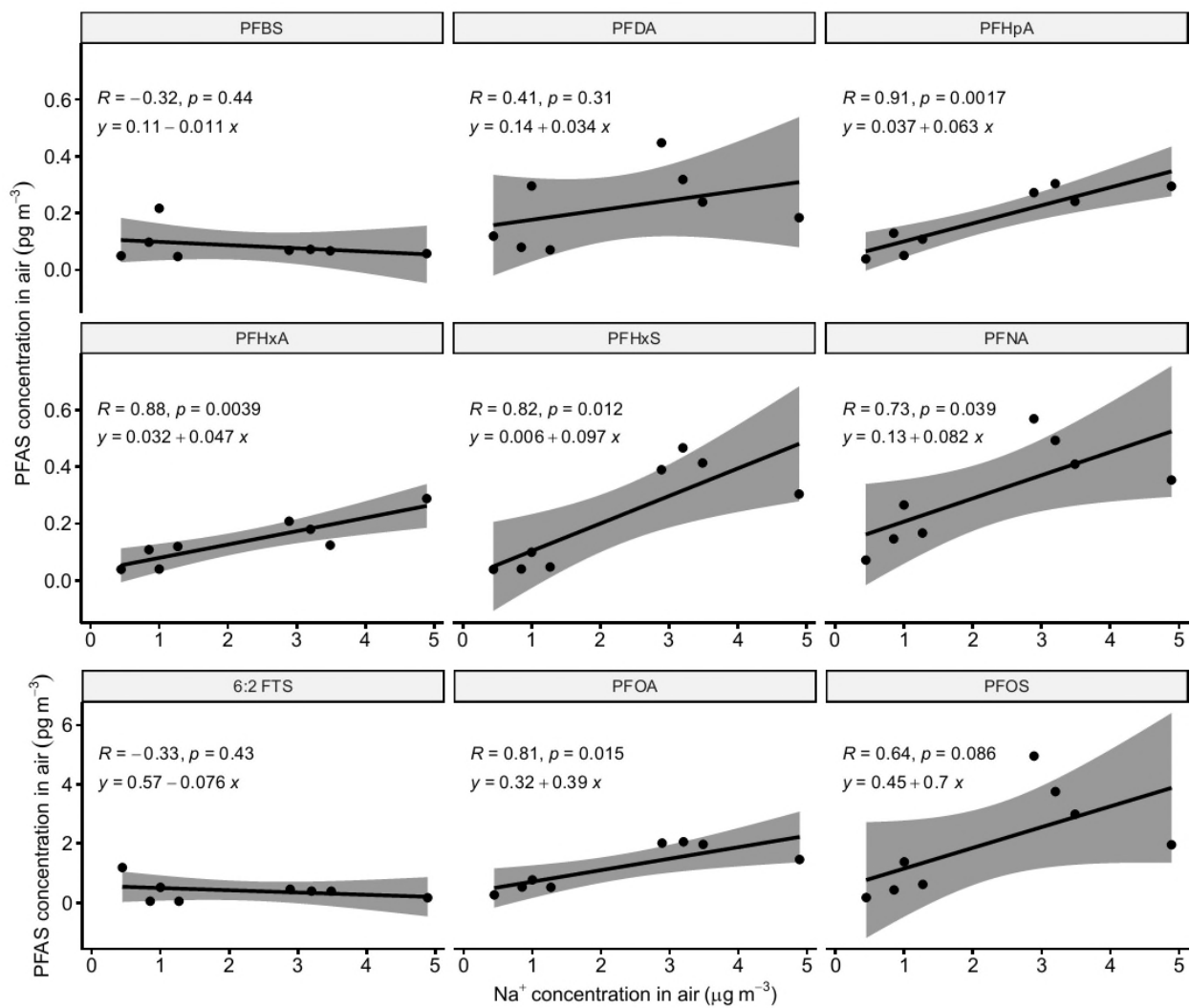


Figure 7. Correlations between Na⁺ and PFAS concentrations measured in SSA collected in Wijk aan Zee (winter and summer combined). The strength of the correlation is estimated by the Pearson correlation coefficient R ($\max = 1$), and the statistical significance of the correlation is indicated by the p -value. Shaded areas indicate confidence intervals of the correlation coefficient at 95%.

For PFOS, the correlation was not statistically significant ($p = 0.086$), although a trend indicating increasing PFOS concentrations for increasing Na⁺ was observed. Poor correlation with Na⁺ may be due to PFAS sources that are not linked to SSA, for instance PFAS present in the gas phase, associated with rain, or transported by continental winds

(see section 3.4). However, due to the limited rainfall, the influence of rain could not be adequately assessed (see table in Annex I). In the case of the precursor 6:2 FTS, photodegradation in the atmosphere might also have contributed to the poor relationship with Na^+ . Among PFCA, PFHxA and PFHpA showed the strongest correlations with Na^+ ($R > 0.88$), and these became progressively weaker with increasing number of carbons starting from PFOA (i.e., $R = 0.81, 0.73$, and 0.41 for PFOA, PFNA and PFDA, respectively). For PFSA, the strongest correlation was found for PFHxS ($R = 0.82$). In samples from Nes, a significant correlation with Na^+ concentrations was observed only for PFNA ($p = 0.0047$), although a general trend showing increasing PFAS concentrations for increasing Na^+ concentrations was observed for PFHpA, PFOA, PFUnDA and PFHxS (Figure 8). This was likely due to the relatively small range of PFAS (and Na^+) concentrations measured in these samples. When data from Wijk aan Zee and Nes were combined, significant correlations were found for all PFAS except for PFBS, 6:2 FTS and PFDA (Figure 9). This may suggest that a larger number of samples is required to adequately assess this relationship.

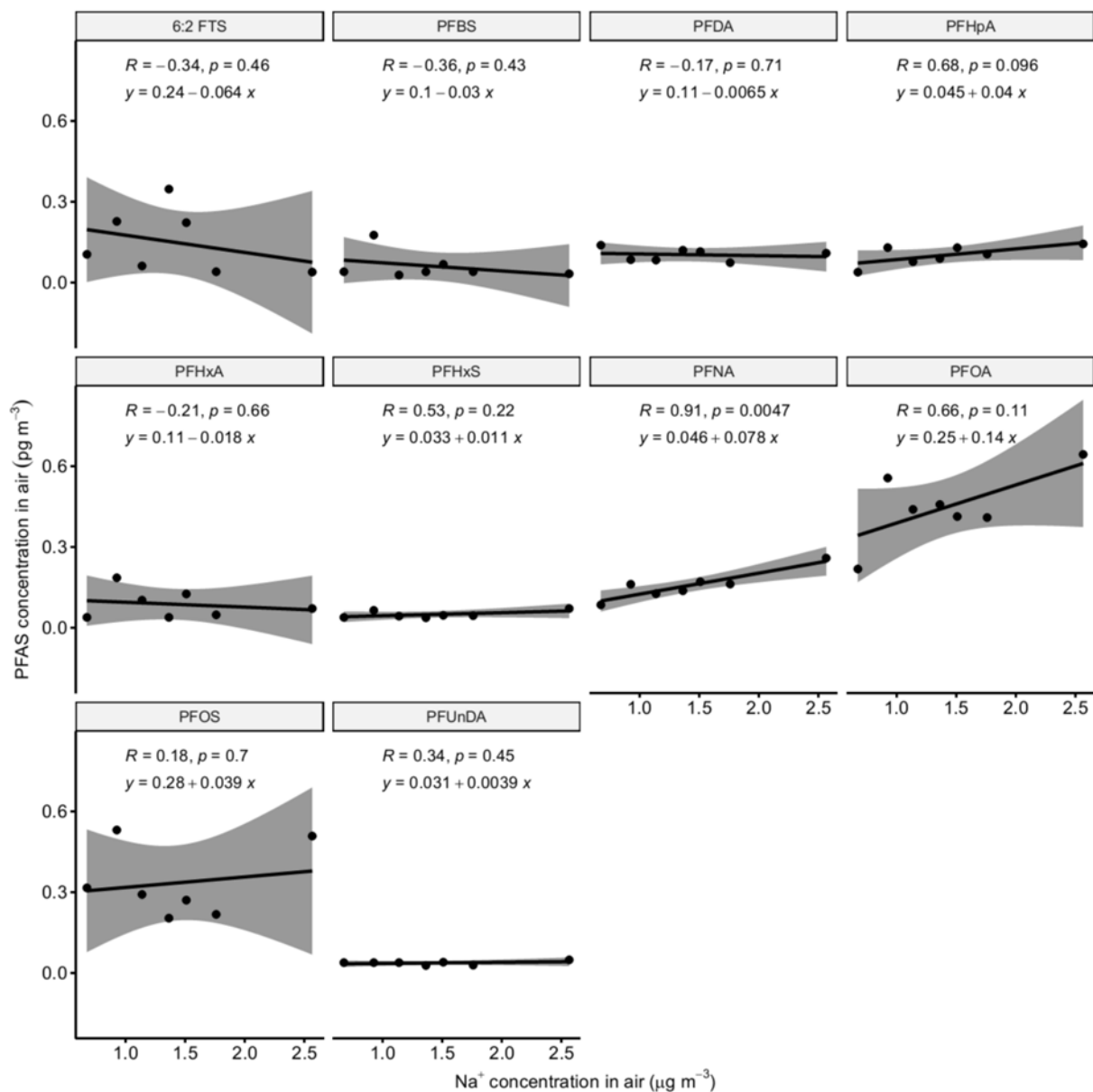


Figure 8. Correlations between Na^+ and PFAS concentrations measured in SSA collected in Nes. The strength of the correlation is estimated by the Pearson correlation coefficient R ($\max = 1$), and the statistical significance of the correlation is indicated by the p -value. Shaded areas indicate confidence intervals of the correlation coefficient at 95%.

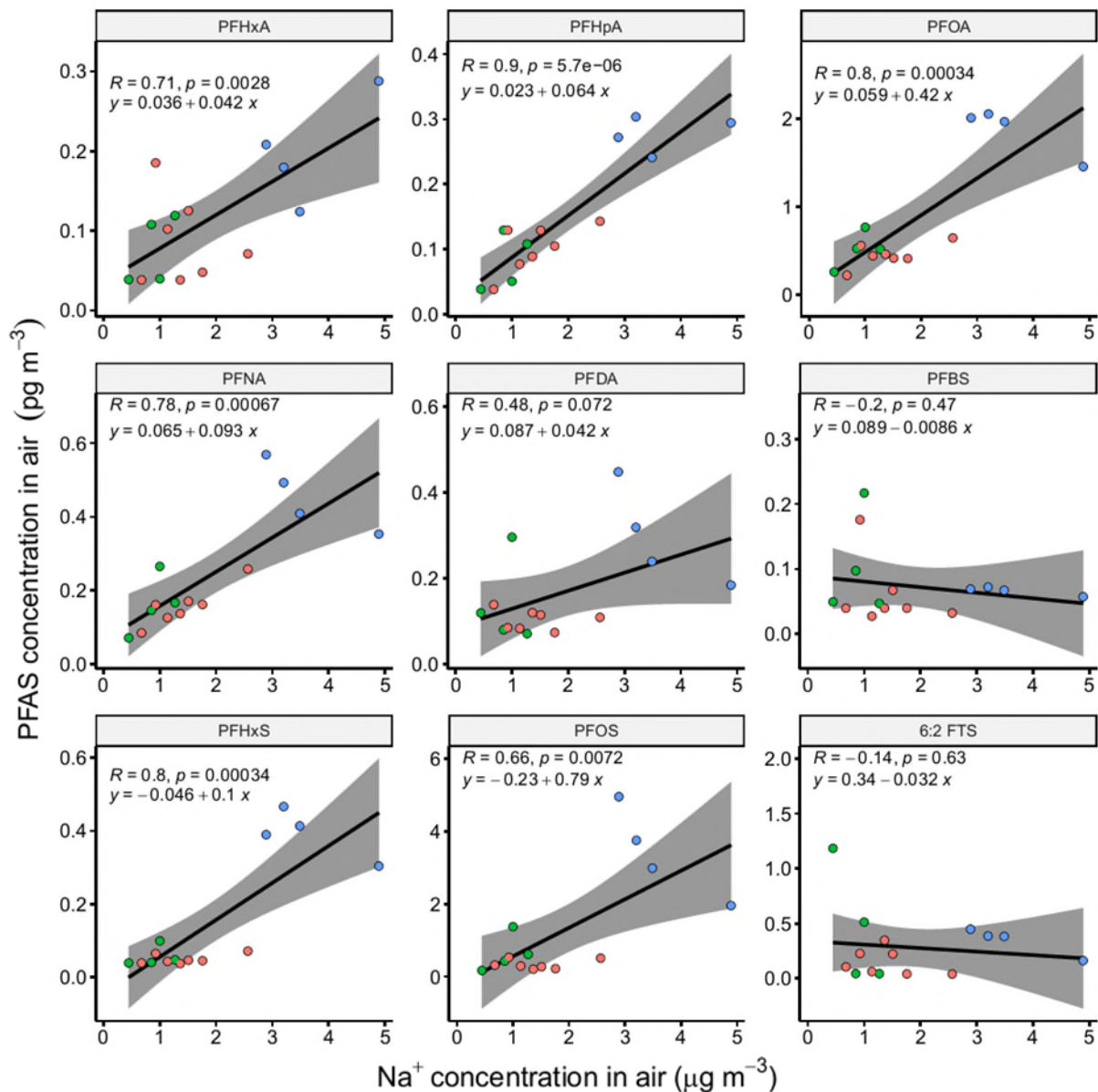


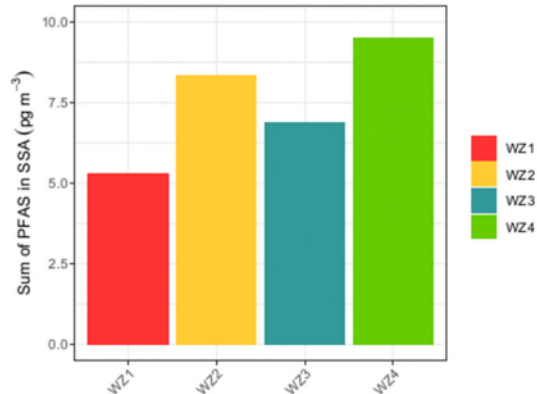
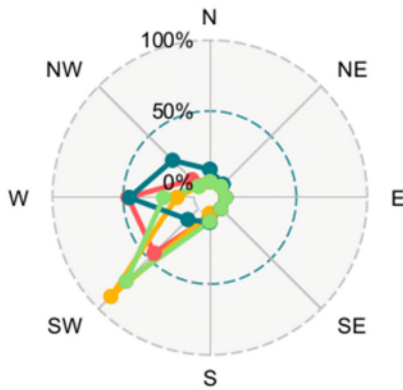
Figure 9. Correlations between Na^+ and combined PFAS concentrations measured in SSA collected in Wijk aan Zee (green and blue for summer and winter samples, respectively) and Nes (red). The strength of the correlation is estimated by the Pearson correlation coefficient R (max = 1), and the statistical significance of the correlation is indicated by the p -value. Shaded areas indicate confidence intervals of the correlation coefficient at 95%.

3.4 Influence of wind direction and speed

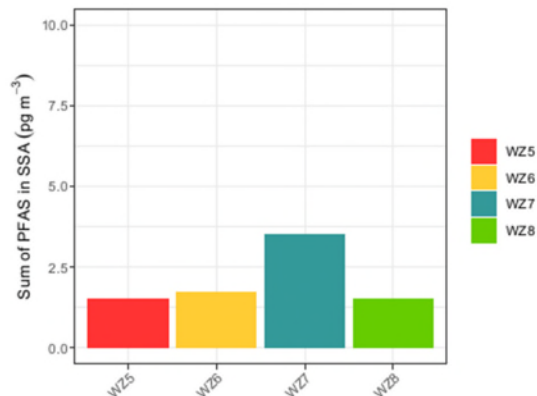
During winter, samples were collected predominately with south-west winds, whereas in summer, samples were mainly collected with north-east winds (Figure 10). In winter, predominantly south-west winds appeared to be associated with higher total concentrations of PFAS than those of predominantly west and north-west winds (total PFAS concentrations were calculated using concentrations > LOQ only). In summer, PFAS concentrations were similar irrespective of the wind direction, except for one sample which showed considerably higher concentrations (WZ7). In Nes, total PFAS concentrations appeared to be higher for samples collected with east, north-east and south-west winds. Winds blowing from the North Sea and the Atlantic Ocean are expected to contain higher concentrations of SSA than those blowing from inland (Figure 2). Differences in Na^+ (and PFAS) concentrations between winds blowing from the sea and from inland could not be adequately assessed due to the small number of samples collected from east and south-east winds. However, samples WZ5 and NE1 were sampled from winds blowing predominately from

east, and showed typically lower concentrations of Na⁺ than those collected from other wind directions (Appendix I). Nevertheless, NE1 showed the highest PFAS concentrations amongst the samples collected in Nes (Figure 10). While some differences in PFAS concentrations were observed between samples collected from different wind directions, PFAS levels did not seem to be linked to specific wind directions, although more samples (including south-east winds) should be collected to adequately assess the potential influence of the wind direction on PFAS atmospheric concentrations, and assess the contribution of additional potential sources of PFAS.

Wijk aan Zee – winter



Wijk aan Zee – summer



Nes – spring

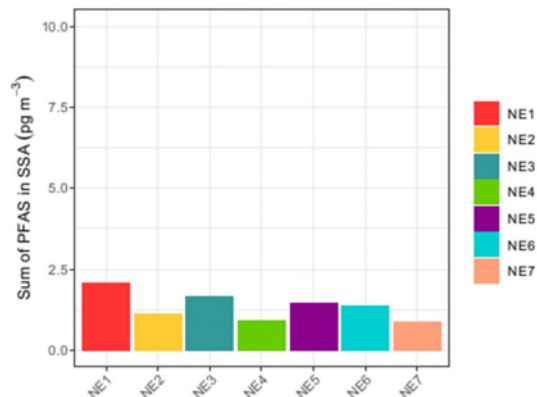
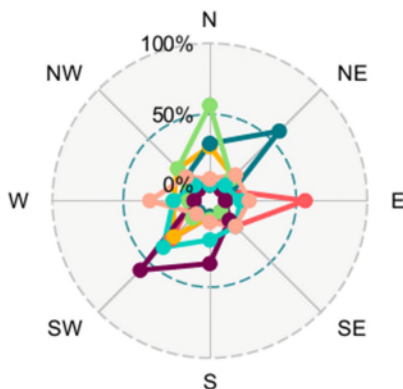


Figure 10. Wind direction recorded during air sampling (left) and total PFAS concentrations measured in the corresponding samples (right).

Strong correlations were also found between PFAS concentrations in air samples and wind speed (Figure 11), except 6:2 FTS and PFBS. Stronger winds generate more waves, and as a consequence, contribute to increased SSA formation. This correlation further indicates that PFAS measured in the atmosphere were linked to SSA.

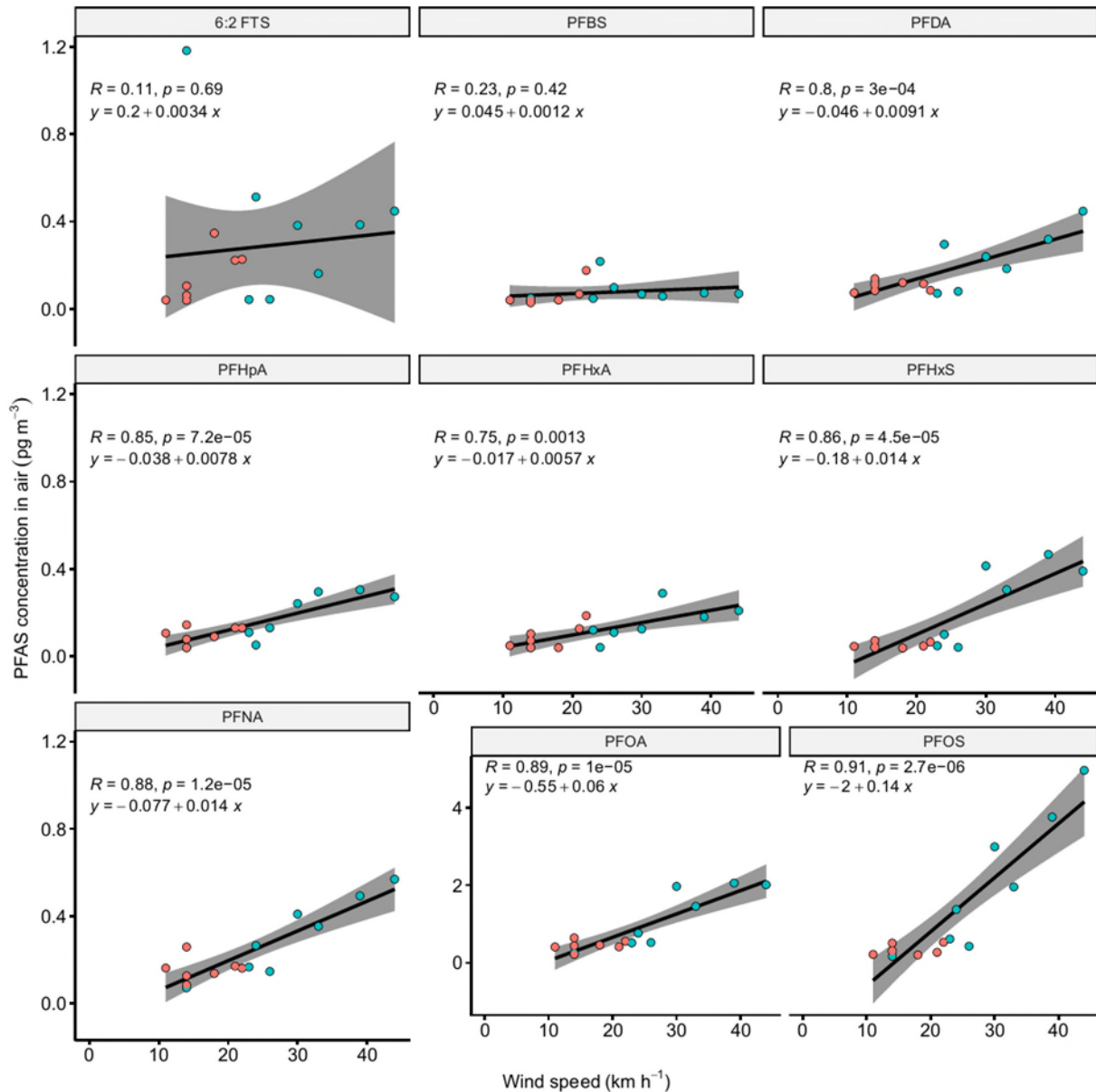


Figure 11. Correlations between wind speed and combined PFAS concentrations measured in air samples collected in Wijk aan Zee (green) and Nes (red). The strength of the correlation is estimated by the Pearson correlation coefficient R (max = 1), and the statistical significance of the correlation is indicated by the p -value. Shaded areas indicate confidence intervals of the correlation coefficient at 95%.

3.5 Concentrations in seawater

The PFAS measured in seawater samples were overall consistent between locations and seasons (Figure 12). Most PFAS were below the LOQ of the method (1 ng/L except PFTeDA and PFTrDA, for which a LOQ of 6 ng/L was applied). Concentrations typically ranged between the LOQ and 3.4 ng/L, except for PFOS in Nes which was found at 12 ng/L. PFNA and PFDA were found only in samples from Nes, whereas HFPO-DA was detected only in Wijk aan Zee during the winter sampling. Except for these 3 compounds, the same PFAS were found in seawater samples irrespective of the locations and season. Concentrations in seawater samples were also very consistent with PFAS concentrations

found in SSA. Concerning PFCAs, compounds from C4 to C10, and from C5 to C11, were found in seawater and SSA, respectively. For PFASs, the same legacy compounds were found in seawater and SSA (i.e., C4, C6 and C8) except for PFHpS which was detected only in SSA (Figure 3). HFPO-DA was found only in Wijk aan Zee during the winter sampling in both seawater and SSA samples. In contrast, 6:2 FTS was consistently found in SSA samples (although frequently below the LOQ), but was not detected in any seawater sample. In combination with the poor correlation found with Na^+ , this may suggest that SSA were unlikely to be a relevant source of 6:2 FTS in the atmosphere. Concentrations of 6:2 FTS appeared to be higher for winds blowing from south-west for both Wijk aan Zee and Nes (Appendix I), however, further research is needed to identify the potential emission source for this compound. In contrast, PFBS was consistently detected in both SSA and seawater samples, however, no significant relationships were found between PFBS and Na^+ concentrations. This suggests that SSA may not be a significant source of atmospheric PFBS at these locations, however, PFBS was frequently measured at concentrations <LOQ, and this may have influenced results.

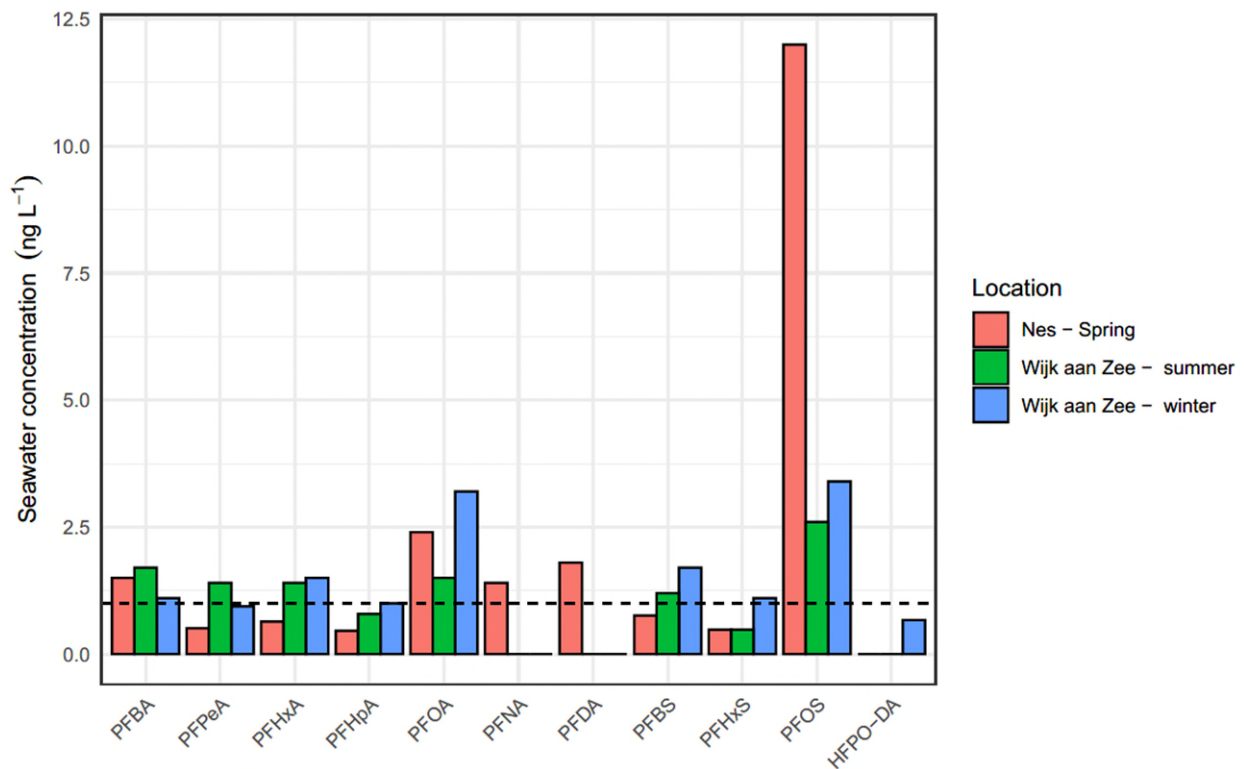


Figure 12. PFAS concentrations in seawater samples collected in different locations and seasons. The horizontal dashed line indicates the LOQ (1 ng/L). Undetected PFAS were not reported in the plot.

3.6 PFAS enrichment in SSA

Enrichment from seawater to SSA has been previously observed for PFAS. Due to their surface-active properties, PFAS are scavenged from seawater by gas bubbles which rise to the seawater-air interface and burst forming SSA. Enrichment factors from (sea)water to SSA ranging from 3 to 5 orders of magnitude have been measured in field and laboratory studies (Cao et al., 2019; H. Johansson et al., 2019; Sha et al., 2021). Enrichment factors in SSA (EF_{SSA}) are calculated using the following equation:

$$EF_{SSA} = \frac{[PFAS]_{SSA}/[Na^+]_{SSA}}{[PFAS]_{seawater}/[Na^+]_{seawater}}$$

where $[PFAS]_{SSA}$ and $[Na^+]_{SSA}$ indicate the concentration of PFAS and Na^+ in SSA, and $[PFAS]_{seawater}$ and $[Na^+]_{seawater}$ the concentration of PFAS and Na^+ in seawater, respectively. In Wijk aan Zee, EF_{SSA} ranged between ~ 20 to ~ 4000 and generally increased with increasing number of carbon atoms (Figure 13), consistently with previous laboratory (H. Johansson et al., 2019; Sha et al., 2021) and field studies (Casas et al., 2020). Temporal variability appeared to show an overall greater enrichment in summer compared to winter at this location. Similar EF_{SSA} were observed in Nes, however, an initial increase in EF_{SSA} with increasing number of carbon atoms was followed by a decrease for PFNA, PFDA, and PFOS.

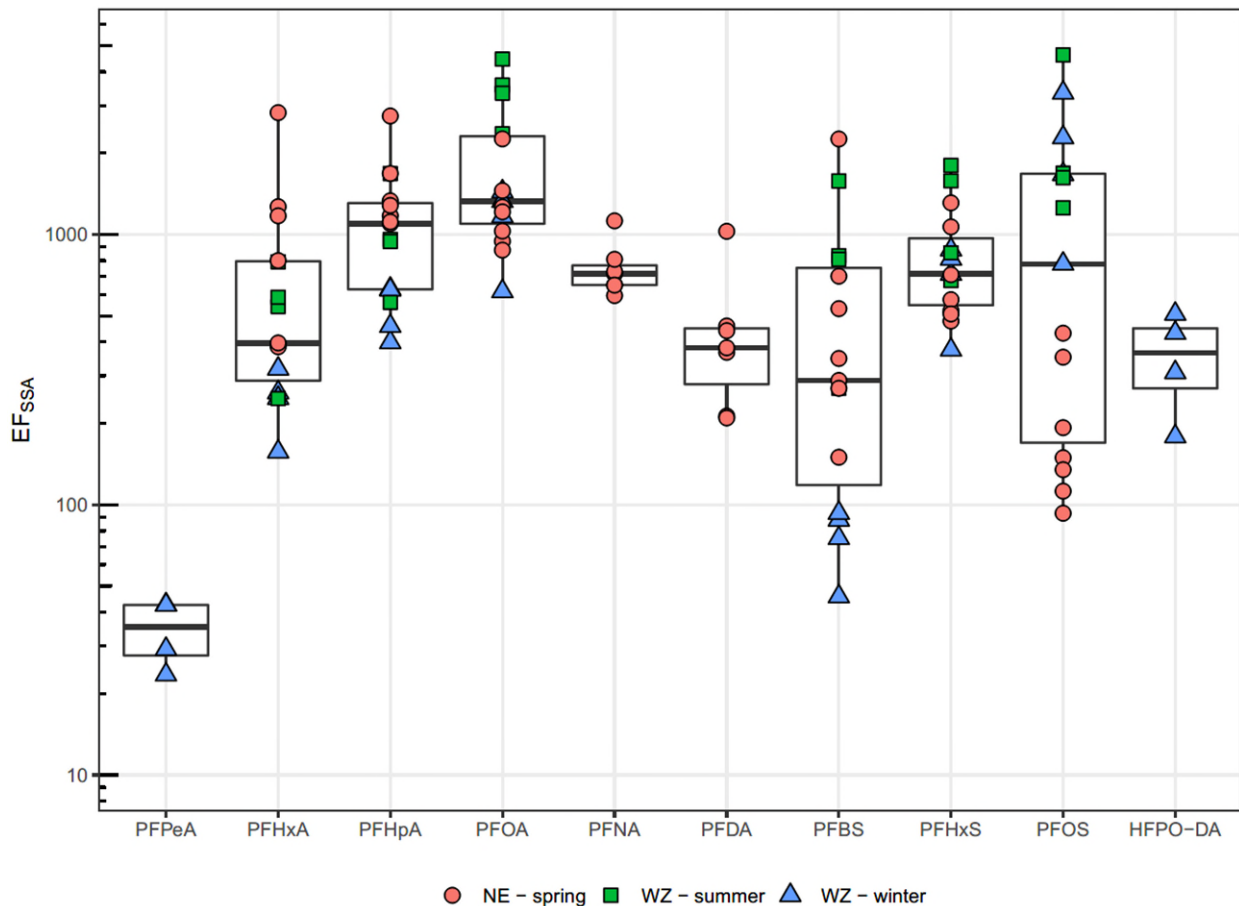


Figure 13. Enrichment factors of PFAS in SSA in the different locations and seasons.

3.7 Indicative estimates of SSA deposition

The atmospheric deposition flux ($pg/m^2/s$) can be calculated from the product of the concentrations measured in the air (pg/m^3) and the deposition velocity (m/s). For aerosols of size similar to that sampled in this study, deposition velocities reported in the literature (mainly for dry deposition) typically range between ~ 0.01 and ~ 0.1 m/s (Ottley and Harrison, 1993; Piskunov, 2009; Zhang et al., 2001; Zheng et al., 2005). However, aerosols deposition velocities vary based on several parameters including wind speed, particle size, humidity, and type of vegetation, thus, more detailed research is needed to accurately estimate deposition velocities at the locations investigated in this study. However, based on the use of 0.01 m/s as a conservative and indicative estimate of deposition velocity, the estimated yearly flux of PFOA and PFOS – obtained by averaging concentrations measured in the different locations and seasons – were 0.27 ± 0.21 and 0.39 ± 0.48 $\mu g/m^2/yr$ ($n = 15$, mean \pm SD), respectively. These estimates were consistent with modelled coastal deposition fluxes reported in the literature (i.e., between 0.05 and 0.4 for PFOA, and between 0.1 and 0.7 for PFOS, respectively) (H. Johansson et al., 2019).

4 Conclusions

PFAS were consistently found in air samples collected from both Wijk aan Zee and Nes. The PFAS composition in the different locations and seasons was very consistent, suggesting that a similar source of PFAS contamination affected these locations. The most abundant compounds found in air samples were PFOA, PFOS, and the precursor 6:2 FTS, although 6:2 FTS concentrations showed large variability and frequently occurred at concentrations < LOQ. PFAS concentrations in air samples collected in Wijk aan Zee were typically from 2 to 7 times higher than those measured in Nes, however, sampling at these locations was performed at different times of the year and differences in PFAS concentrations may be due to spatial as well as temporal (i.e., seasonal) variability. Measurements performed in Wijk aan Zee in winter were higher than those measured in summer, suggesting seasonal variability in PFAS concentrations at this location. Na^+ and Mg^{2+} were consistently found in air samples (at ratios consistent with those measured in seawater), indicating the presence of SSA in the atmosphere. Significant relationships were found between PFAS and Na^+ concentrations measured in air samples (except for PFBS, 6:2 FTS and PFDA), suggesting that SSA were a major source of PFAS in air. However, it is unclear what factors may have contributed to the poor relationships observed for PFBS and 6:2 FTS; PFBS has a relatively short carbon chain (C4) and low surface activity, and this may affect its adsorption on air bubbles; 6:2 FTS is widely used as a replacement of legacy PFAS and additional sources that are not linked to SSA may have contributed to its levels in the atmosphere. The relationship between PFDA and Na^+ was not statistically significant (i.e., $p = 0.072$, which is greater than the significance level 0.05), however, still much stronger than that of PFBS ($p = 0.47$) and 6:2 FTS ($p = 0.63$).

Additional sampling is required to establish stronger relationships between SSA and PFAS contamination in air, and investigate the occurrence of additional sources of atmospheric PFAS at these locations. PFAS concentrations in SSA were overall consistent with those measured in seawater, and were shown to be enriched up to 4000 times in SSA. These enrichment factors may be used to estimate PFAS concentrations in SSA based on seawater concentrations (assuming constant Na^+ concentrations in seawater and Na^+ concentrations in SSA within the range measured in this study).

Overall, these preliminary results suggest that PFAS are present in SSA collected along the Dutch coastline and that SSA may be a major source of PFAS contamination in air, further strengthening the hypothesis that SSA plays a role in the transport and deposition of PFAS along the coast. In addition, a previous study from RIVM showed that sea salt is detected in the atmosphere across the whole of the Netherlands, suggesting that SSA may potentially affect areas also further inland (Appendix I). Additional studies investigating PFAS concentrations (and behavior) in soil are needed to determine the extent of PFAS deposition via SSA and its potential contribution to the contamination of groundwater used for drinking water production at these sites.

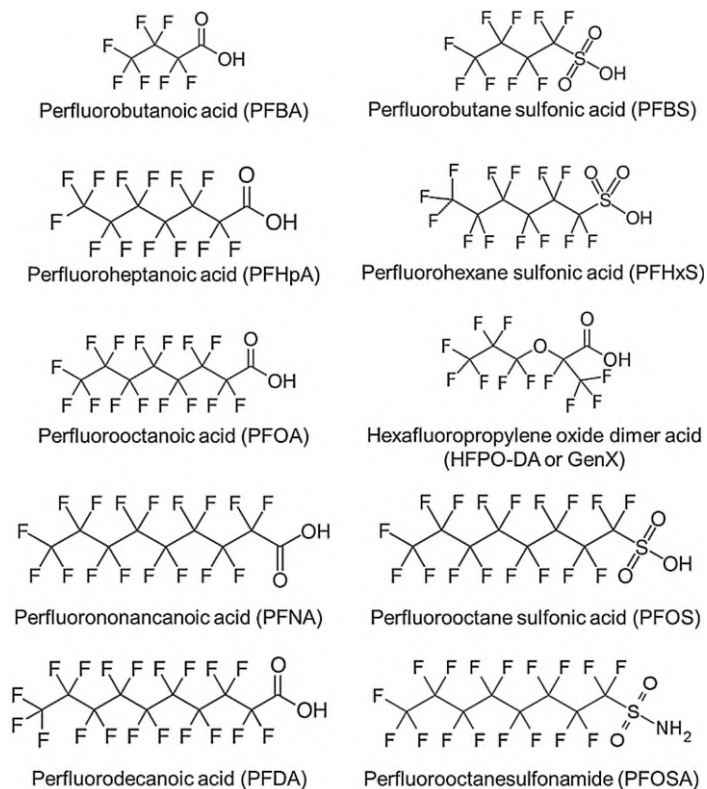
References

- Ahrens, L., Norström, K., Viktor, T., Cousins, A.P., Josefsson, S., 2015. Stockholm Arlanda Airport as a source of per- and polyfluoroalkyl substances to water, sediment and fish. *Chemosphere, Per- and Polyfluorinated Alkyl substances (PFASs) in materials, humans and the environment – current knowledge and scientific gaps*. 129, 33–38. <https://doi.org/10.1016/j.chemosphere.2014.03.136>
- Ateia, M., Maroli, A., Tharayil, N., Karanfil, T., 2019. The overlooked short- and ultrashort-chain poly- and perfluorinated substances: A review. *Chemosphere* 220, 866–882. <https://doi.org/10.1016/j.chemosphere.2018.12.186>
- Balگووین, S., Remucal, C.K., 2022. Tributary Loading and Sediment Desorption as Sources of PFAS to Receiving Waters. *ACS EST Water*. <https://doi.org/10.1021/acsestwater.1c00348>
- Cao, Y., Lee, C., Davis, E.T.J., Si, W., Wang, F., Trimpin, S., Luo, L., 2019. 1000-Fold Preconcentration of Per- and Polyfluorinated Alkyl Substances within 10 Minutes via Electrochemical Aerosol Formation. *Anal. Chem.* 91, 14352–14358. <https://doi.org/10.1021/acs.analchem.9b02758>
- Casal, P., Zhang, Y., Martin, J.W., Pizarro, M., Jiménez, B., Dachs, J., 2017. Role of Snow Deposition of Perfluoroalkylated Substances at Coastal Livingston Island (Maritime Antarctica). *Environ. Sci. Technol.* 51, 8460–8470. <https://doi.org/10.1021/acs.est.7b02521>
- Casas, G., Martínez-Varela, A., Roscales, J.L., Vila-Costa, M., Dachs, J., Jiménez, B., 2020. Enrichment of perfluoroalkyl substances in the sea-surface microlayer and sea-spray aerosols in the Southern Ocean. *Environ. Pollut.* 267, 115512. <https://doi.org/10.1016/j.envpol.2020.115512>
- Cousins, I.T., Vestergren, R., Wang, Z., Scheringer, M., McLachlan, M.S., 2016. The precautionary principle and chemicals management: The example of perfluoroalkyl acids in groundwater. *Environ. Int.* 94, 331–340. <https://doi.org/10.1016/j.envint.2016.04.044>
- Culkin, F., Cox, R.A., 1966. Sodium, potassium, magnesium, calcium and strontium in sea water. *Deep Sea Res. Oceanogr. Abstr.* 13, 789–804. [https://doi.org/10.1016/0011-7471\(76\)90905-0](https://doi.org/10.1016/0011-7471(76)90905-0)
- de Leeuw, G., Andreas, E.L., Anguelova, M.D., Fairall, C.W., Lewis, E.R., O'Dowd, C., Schulz, M., Schwartz, S.E., 2011. Production flux of sea spray aerosol. *Rev. Geophys.* 49. <https://doi.org/10.1029/2010RG000349>
- Hamid, H., Li, L.Y., Grace, J.R., 2018. Review of the fate and transformation of per- and polyfluoroalkyl substances (PFASs) in landfills. *Environ. Pollut.* 235, 74–84. <https://doi.org/10.1016/j.envpol.2017.12.030>
- H. Johansson, J., E. Salter, M., Navarro, J.C.A., Leck, C., D. Nilsson, E., T. Cousins, I., 2019. Global transport of perfluoroalkyl acids via sea spray aerosol. *Environ. Sci. Process. Impacts* 21, 635–649. <https://doi.org/10.1039/C8EM00525G>
- Lai, F.Y., Rauert, C., Gobelius, L., Ahrens, L., 2019. A critical review on passive sampling in air and water for per- and polyfluoroalkyl substances (PFASs). *TrAC Trends Anal. Chem.* 121, 115311. <https://doi.org/10.1016/j.trac.2018.11.009>
- Langberg, H.A., Breedveld, G.D., Slinde, G.A., Grønning, H.M., Høisæter, Å., Jartun, M., Rundberget, T., Jenssen, B.M., Hale, S.E., 2020. Fluorinated Precursor Compounds in Sediments as a Source of Perfluorinated Alkyl Acids (PFAA) to Biota. *Environ. Sci. Technol.* 54, 13077–13089. <https://doi.org/10.1021/acs.est.0c04587>
- Melake, B.A., Bervoets, L., Nkuba, B., Groffen, T., 2022. Distribution of perfluoroalkyl substances (PFASs) in water, sediment, and fish tissue, and the potential human health risks due to fish consumption in Lake Hawassa, Ethiopia. *Environ. Res.* 204, 112033. <https://doi.org/10.1016/j.envres.2021.112033>
- Muir, D., Miaz, L.T., 2021. Spatial and Temporal Trends of Perfluoroalkyl Substances in Global Ocean and Coastal Waters. *Environ. Sci. Technol.* 55, 9527–9537. <https://doi.org/10.1021/acs.est.0c08035>
- Mullin, L., Katz, D.R., Riddell, N., Plumb, R., Burgess, J.A., Yeung, L.W.Y., Jogsten, I.E., 2019. Analysis of hexafluoropropylene oxide-dimer acid (HFPO-DA) by liquid chromatography-mass spectrometry (LC-MS): Review of current approaches and environmental levels. *TrAC Trends Anal. Chem.* 118, 828–839. <https://doi.org/10.1016/j.trac.2019.05.015>
- Oppo, C., Bellandi, S., Degli Innocenti, N., Stortini, A.M., Loglio, G., Schiavuta, E., Cini, R., 1999. Surfactant components of marine organic matter as agents for biogeochemical fractionation and pollutant transport via marine aerosols. *Mar. Chem.* 63, 235–253. [https://doi.org/10.1016/S0304-4203\(98\)00065-6](https://doi.org/10.1016/S0304-4203(98)00065-6)
- Ottley, C.J., Harrison, R.M., 1993. Atmospheric dry deposition flux of metallic species to the North Sea. *Atmospheric Environ. Part Gen. Top.* 27, 685–695. [https://doi.org/10.1016/0960-1686\(93\)90187-4](https://doi.org/10.1016/0960-1686(93)90187-4)
- Piskunov, V.N., 2009. Parameterization of aerosol dry deposition velocities onto smooth and rough surfaces. *J. Aerosol Sci.* 40, 664–679. <https://doi.org/10.1016/j.jaerosci.2009.04.006>

- Podder, A., Sadmani, A.H.M.A., Reinhart, D., Chang, N.-B., Goel, R., 2021. Per and poly-fluoroalkyl substances (PFAS) as a contaminant of emerging concern in surface water: A transboundary review of their occurrences and toxicity effects. *J. Hazard. Mater.* 419, 126361. <https://doi.org/10.1016/j.jhazmat.2021.126361>
- Reth, M., Berger, U., Broman, D., Cousins, I.T., Nilsson, E.D., McLachlan, M.S., Reth, M., Berger, U., Broman, D., Cousins, I.T., Nilsson, E.D., McLachlan, M.S., 2011. Water-to-air transfer of perfluorinated carboxylates and sulfonates in a sea spray simulator. *Environ. Chem.* 8, 381–388. <https://doi.org/10.1071/EN11007>
- RIVM, 2012. Assessment of the level of sea salt in PM10 in the Netherlands (No. 680704014).
- Sammut, G., Sinagra, E., Helmus, R., de Voogt, P., 2017. Perfluoroalkyl substances in the Maltese environment – (I) surface water and rain water. *Sci. Total Environ.* 589, 182–190. <https://doi.org/10.1016/j.scitotenv.2017.02.128>
- Sha, B., Johansson, J.H., Benskin, J.P., Cousins, I.T., Salter, M.E., 2021. Influence of Water Concentrations of Perfluoroalkyl Acids (PFAAs) on Their Size-Resolved Enrichment in Nascent Sea Spray Aerosols. *Environ. Sci. Technol.* 55, 9489–9497. <https://doi.org/10.1021/acs.est.0c03804>
- Sha, B., Johansson, J.H., Tunved, P., Bohlin-Nizzetto, P., Cousins, I.T., Salter, M.E., 2022. Sea Spray Aerosol (SSA) as a Source of Perfluoroalkyl Acids (PFAAs) to the Atmosphere: Field Evidence from Long-Term Air Monitoring. *Environ. Sci. Technol.* 56, 228–238. <https://doi.org/10.1021/acs.est.1c04277>
- Sharma, B.M., Bharat, G.K., Tayal, S., Larssen, T., Bečanová, J., Karásková, P., Whitehead, P.G., Futter, M.N., Butterfield, D., Nizzetto, L., 2016. Perfluoroalkyl substances (PFAS) in river and ground/drinking water of the Ganges River basin: Emissions and implications for human exposure. *Environ. Pollut.* 208, 704–713. <https://doi.org/10.1016/j.envpol.2015.10.050>
- Shimizu, M.S., Mott, R., Potter, A., Zhou, J., Baumann, K., Surratt, J.D., Turpin, B., Avery, G.B., Harfmann, J., Kieber, R.J., Mead, R.N., Skrabal, S.A., Willey, J.D., 2021. Atmospheric Deposition and Annual Flux of Legacy Perfluoroalkyl Substances and Replacement Perfluoroalkyl Ether Carboxylic Acids in Wilmington, NC, USA. *Environ. Sci. Technol. Lett.* 8, 366–372. <https://doi.org/10.1021/acs.estlett.1c00251>
- Sunderland, E.M., Hu, X.C., Dassuncao, C., Tokranov, A.K., Wagner, C.C., Allen, J.G., 2019. A review of the pathways of human exposure to poly- and perfluoroalkyl substances (PFASs) and present understanding of health effects. *J. Expo. Sci. Environ. Epidemiol.* 29, 131–147. <https://doi.org/10.1038/s41370-018-0094-1>
- Tang, A., Zhang, X., Li, R., Tu, W., Guo, H., Zhang, Y., Li, Z., Liu, Y., Mai, B., 2022. Spatiotemporal distribution, partitioning behavior and flux of per- and polyfluoroalkyl substances in surface water and sediment from Poyang Lake, China. *Chemosphere* 295, 133855. <https://doi.org/10.1016/j.chemosphere.2022.133855>
- Thai, P.K., McDonough, J.T., Key, T.A., Thompson, J., Prasad, P., Porman, S., Mueller, J.F., 2022. Release of perfluoroalkyl substances from AFFF-impacted concrete in a firefighting training ground (FTG) under repeated rainfall simulations. *J. Hazard. Mater. Lett.* 3, 100050. <https://doi.org/10.1016/j.hazl.2022.100050>
- Van Leeuwen, J., Stofberg, S., Grift, B. van der, Hartog, N., 2023. Verkenning uitspoeling van diffuse PFAS verontreiniging voor onverzadigde bodems in Nederland. KWR 2023.029.
- Weber, A.K., Barber, L.B., LeBlanc, D.R., Sunderland, E.M., Vecitis, C.D., 2017. Geochemical and Hydrologic Factors Controlling Subsurface Transport of Poly- and Perfluoroalkyl Substances, Cape Cod, Massachusetts. *Environ. Sci. Technol.* 51, 4269–4279. <https://doi.org/10.1021/acs.est.6b05573>
- Wong, F., Shoeib, M., Katsoyiannis, A., Eckhardt, S., Stohl, A., Bohlin-Nizzetto, P., Li, H., Fellin, P., Su, Y., Hung, H., 2018. Assessing temporal trends and source regions of per- and polyfluoroalkyl substances (PFASs) in air under the Arctic Monitoring and Assessment Programme (AMAP). *Atmos. Environ.* 172, 65–73. <https://doi.org/10.1016/j.atmosenv.2017.10.028>
- Wu, C., Wang, Q., Chen, H., Li, M., 2022. Rapid quantitative analysis and suspect screening of per- and polyfluorinated alkyl substances (PFASs) in aqueous film-forming foams (AFFFs) and municipal wastewater samples by Nano-ESI-HRMS. *Water Res.* 219, 118542. <https://doi.org/10.1016/j.watres.2022.118542>
- Yang, L.-H., Yang, W.-J., Lv, S.-H., Zhu, T.-T., Adeel Sharif, H.M., Yang, C., Du, J., Lin, H., 2022. Is HFPO-DA (GenX) a suitable substitute for PFOA? A comprehensive degradation comparison of PFOA and GenX via electrooxidation. *Environ. Res.* 204, 111995. <https://doi.org/10.1016/j.envres.2021.111995>
- Young, C.J., Furdui, V.I., Franklin, J., Koerner, R.M., Muir, D.C.G., Mabury, S.A., 2007. Perfluorinated Acids in Arctic Snow: New Evidence for Atmospheric Formation. *Environ. Sci. Technol.* 41, 3455–3461. <https://doi.org/10.1021/es0626234>
- Zhang, L., Gong, S., Padro, J., Barrie, L., 2001. A size-segregated particle dry deposition scheme for an atmospheric aerosol module. *Atmos. Environ.* 35, 549–560. [https://doi.org/10.1016/S1352-2310\(00\)00326-5](https://doi.org/10.1016/S1352-2310(00)00326-5)

- Zhao, P., Xia, X., Dong, J., Xia, N., Jiang, X., Li, Y., Zhu, Y., 2016. Short- and long-chain perfluoroalkyl substances in the water, suspended particulate matter, and surface sediment of a turbid river. *Sci. Total Environ.* 568, 57–65. <https://doi.org/10.1016/j.scitotenv.2016.05.221>
- Zheng, M., Guo, Z., Fang, M., Rahn, K.A., Kester, D.R., 2005. Dry and wet deposition of elements in Hong Kong. *Mar. Chem.*, Special Issue in honor of Dana R. Kester 97, 124–139. <https://doi.org/10.1016/j.marchem.2005.05.007>

Appendix I



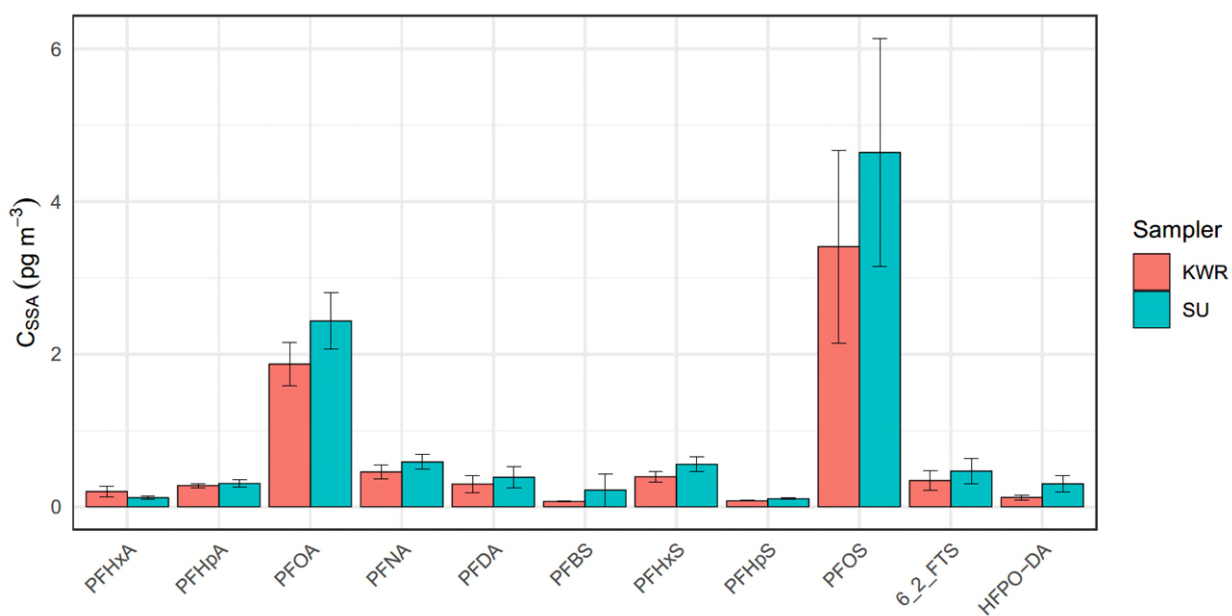
Examples of PFAS chemical structures.



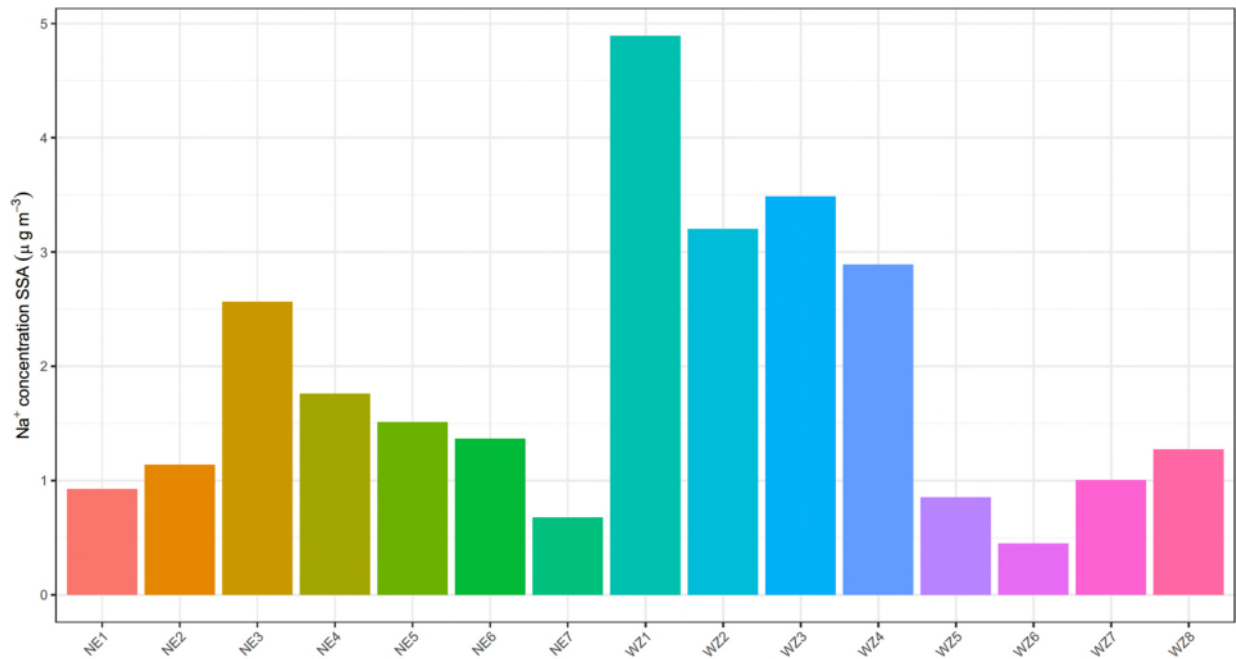
Picture of the high-volume air samplers provided by Stockholm University (left) and KWR (right) for sampling in Wijk aan Zee.

Atmospheric parameters measured during air sampling.

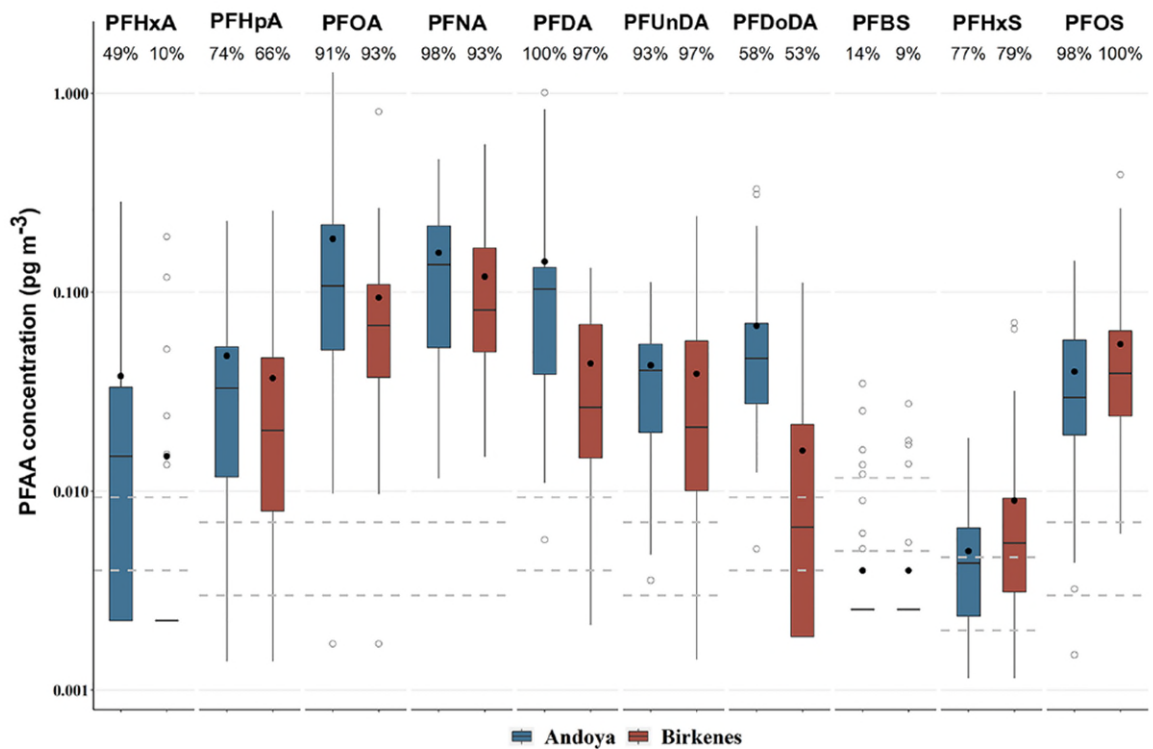
		Wind speed		Temperature		Total rainfall		Rainfall intensity	Humidity	
		km/h		°C	h	mm	mm/h	%		
Wijk aan Zee	<i>Winter</i>									
	WZ1	33	± 11	7.9	± 0.5	0.9	0.3	0.3	89	± 6
	WZ2	39	± 5	7.9	± 0.8	0.7	0.1	0.1	87	± 7
	WZ3	30	± 14	6.5	± 0.8	7.4	4.8	0.6	79	± 15
	WZ4	44	± 12	7.8	± 1.0	9.4	10.4	1.1	87	± 7
	<i>Summer</i>									
	WZ5	26	± 5	16.5	± 2.6	0.0	0.0	-	65	± 13
	WZ6	14	± 4	21.5	± 2.3	0.0	0.0	-	74	± 11
WZ7	24	± 8	21.8	± 3.3	1.1	1.4	1.3	78	± 16	
WZ8	23	± 6	16.5	± 3.2	0.0	0.0	-	74	± 12	
Nes	<i>Spring</i>									
	NE1	22	± 9	10.4	± 2.8	0.0	0.0	-	80	± 10
	NE2	14	± 4	9.2	± 2.3	0.0	0.0	-	88	± 6
	NE3	14	± 4	8.1	± 1.1	0.0	0.0	-	73	± 5
	NE4	11	± 6	8.9	± 1.8	0.0	0.0	-	73	± 12
	NE5	21	± 9	14.6	± 1.7	1.1	0.8	0.7	79	± 12
	NE6	18	± 6	16.7	± 2.1	0.0	0.0	-	82	± 11
NE7	14	± 7	14.0	± 3.3	5.3	31.5	5.9	91	± 9	



PFAS concentrations measured in SSA collected using the sampler from KWR and Stockholm University (mean \pm SD, n = 4)

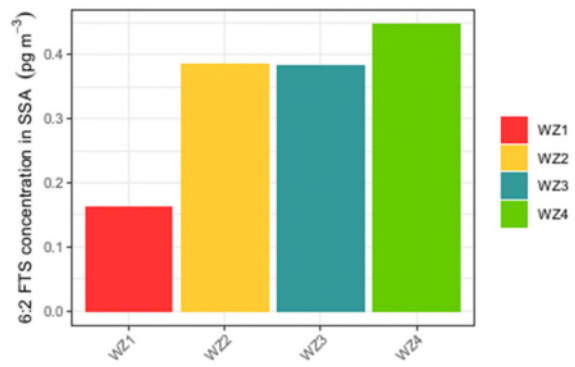
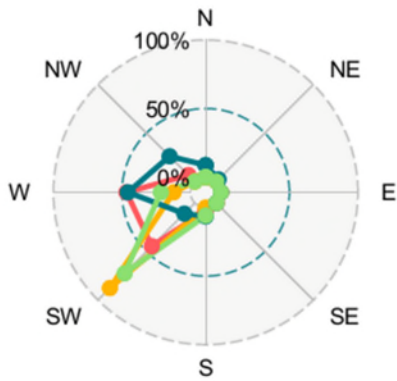


Sodium concentrations measured in air samples from Nes (NE1-NE7) and Wijk aan Zee (WZ1-WZ8).

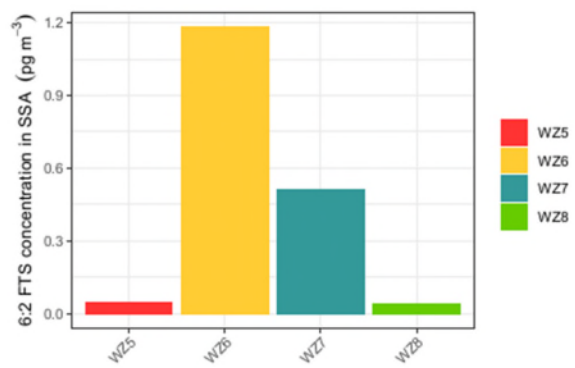
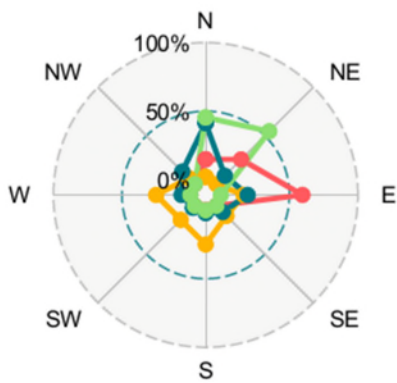


PFAS concentrations measured in SSA collected in Andoya and Birkenes, Norway, between April 2018 and July 2020 (Sha et al., 2022).

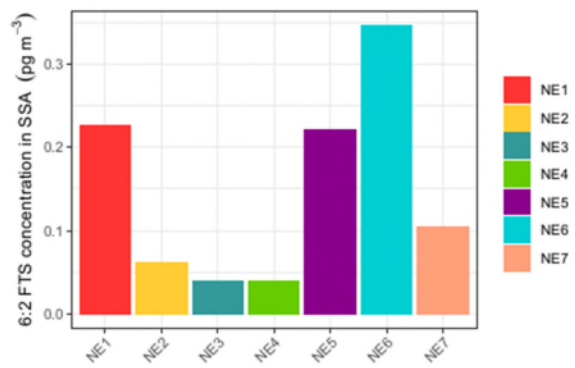
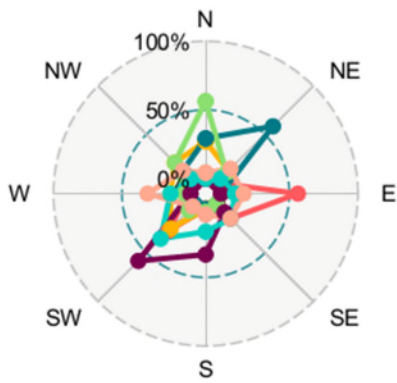
Wijk aan Zee – winter



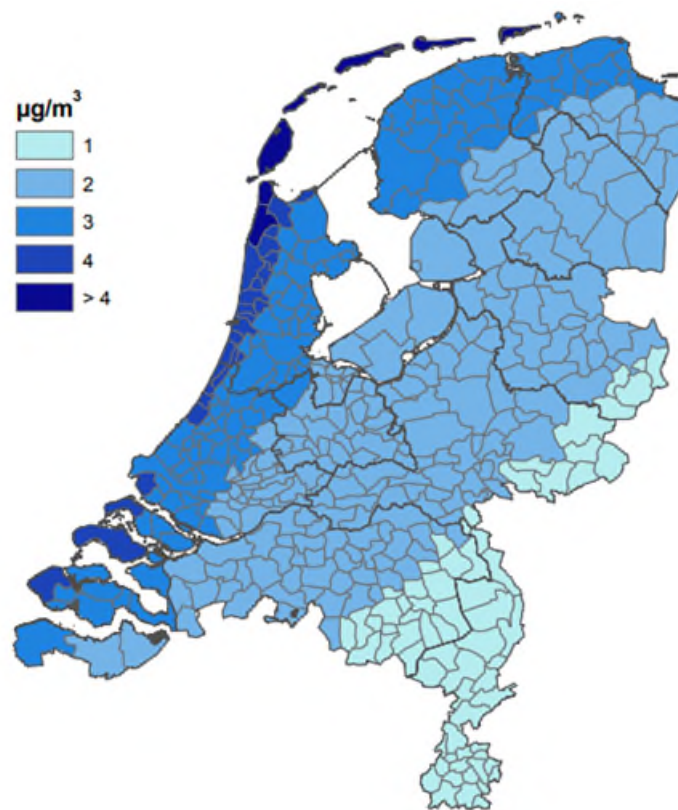
Wijk aan Zee – summer



Nes – spring



Wind direction recorded during air sampling (left) and 6:2 FTS concentrations measured in the corresponding samples (right).



Modelled average sea salt concentration for the period 2008-2010. The results are geographically averaged for each municipality. Sea salt concentrations are obtained by multiplying the concentration of Na^+ in the atmosphere times 3.26 (RIVM, 2012).